Chapter 8
Climate Change Impacts to Hurricane-Induced Wind and Storm Surge Losses for Three Major Metropolitan Regions in the U.S.

Peter J. Sousounis, Roger Grenier, Jonathan Schneyer, and Dan Raizman

Abstract Climate change is expected to have increasingly significant impacts on U.S. hurricane activity through this century (Hayhoe et al., Our changing climate. In: Reidmiller DR, Avery CW, Easterling DR, Kunkel KE, Lewis KLM, Maycock TK, Stewart BC (eds) Impacts, risks, and adaptation in the United States: fourth national climate assessment, volume II. U.S. Global Change Research Program, Washington, DC, pp 72:144. https://doi.org/10.7930/NCA4.2018.CH, 2018). A key concern for private insurers is how the relative contributions to loss from wind and water may change because damage from flood is not typically covered in the residential market. This study addresses the concern by considering how climate change by 2050 under an extreme climate scenario may impact hurricane frequency and damage. Using a stochastic catalog of 100,000 years of possible events that can occur in today's climate, and available information on how hurricane frequency and intensity may change, multiple catalogs of events are created to reflect future hurricane activity. Climate change impacts on precipitation rate are not accounted for here, although sea level rise is included to understand how much worse storm surge may become. Relative changes to wind loss and coastal flood loss are examined for three economically significant and hurricane prone urban locations: Houston-Galveston, Miami, and New York. Results show that relative changes in wind loss may pale in comparison to relative changes in storm surge loss. Houston shows large increases in relative contribution of surge to total loss because the contribution is currently small, New York shows the least significant increases because contributions are currently large, and Miami is in the middle.

P. J. Sousounis (✉) · R. Grenier · D. Raizman
AIR Worldwide, Boston, MA, USA
e-mail: psousounis@air-worldwide.com; rgrenier@air-worldwide.com; draizman@air-worldwide.com

J. Schneyer
Willis Re, Boston, MA, USA
e-mail: jonathan.schneyer@rsmas.miami.edu

J. M. Collins, J. M. Done (eds.), *Hurricane Risk in a Changing Climate*,
Hurricane Risk 2, https://doi.org/10.1007/978-3-031-08568-0_8

Keywords Hurricane · Climate change · Storm surge · Sea level rise

8.1 Introduction

Climate change is expected to have significant impacts on hurricanes and the damage they cause by the end of this century (Hayhoe et al. 2018). Even by mid-century, the windspeeds and storm surge inundation heights and extents may be greater than what the U.S. coastline is exposed to at present (Villarini and Vecchi 2013; Little et al. 2015). Moreover, the relative changes in damage to property from wind, storm surge, and precipitation-induced flooding may not be equal. Increases in storm surge damage from rising seas, along with increasing damage further inland due to precipitation-induced inland flooding from the Clausius Clapeyron effect (Liu et al. 2019), may outpace increases in wind damage. Arctic amplification is contributing significantly to melting of the Greenland ice sheet (Hofer et al. 2020) and global warming in general is heating and expanding ocean water. Sea levels have risen globally on average some 10 cm in the last 50 years (Frederikse et al. 2020), but along some portions of the U.S. coastline, sea levels have experienced two to three times that equivalent rate of rise in the last 15 years. (e.g., Ocean City, MD has experienced 6 mm/year of sea level rise according to data from NOAA 2021). Other factors, like a slowdown in the Atlantic Meridional Overturning Circulation (Caesar et al. 2021), which is contributing to sea level rise (SLR), may also be related to climate change.

The physics and thermodynamics of melting ice contributing to SLR may be relatively straightforward compared to how climate change may affect hurricane intensity. Increasing sea surface temperatures (SSTs) certainly contribute to an increase in the potential intensity of a storm but how outflow temperature, vertical wind shear, and distribution of moisture (to name a few) may change are less well understood and may counter some of the potential intensity increases from increased SSTs. How the relative risks may change in the future are especially important considering that damage from (coastal) flood for residential property is not typically insured by private carriers and is underinsured in general, contributing to a "protection gap" where losses are borne by individuals, businesses, and taxpayers.

The topic for this study is directly motivated by increasing concerns from the insurance industry regarding how climate change may impact hurricane losses. Companies that develop catastrophe models for use by the insurance industry are being asked quite frequently if not only do the models that they provide account for climate change for the short time horizons that insurance companies typically focus on but whether catastrophe models can provide a view of the risk on longer time horizons.

A previous similar study (Grenier et al. 2020) focused on total loss from all hurricane-related sub-perils combined. In this study, we consider how climate change by mid-century may impact hurricane wind and coastal flood risk separately. Specific attention is paid to how the relative breakdown of wind losses vs. surge

losses may change. The relative breakdown is a concern from an insurance standpoint because residential flood damage is not a risk that is typically insured by commercial insurance companies. Coverage is available through the National Flood Insurance Program (NFIP), although take-up is low (NAIC 2017), especially outside of designated special flood hazard areas. Although risk from inland flood is also likely to increase because of higher atmospheric moisture content, stronger horizontal moisture convergence associated with stronger hurricanes (Liu et al. 2019), and possibly slower moving storms (Hall and Kossin 2019), we do not explicitly evaluate the impact from a change in that risk in this paper.

The basic methodology that is used leverages the AIR Worldwide Hurricane Model for the United States (hereafter AIR Hurricane Model). This is a proprietary model, although some good information is publicly available from the State Board of Administration of Florida (AIR 2021) and from Grenier et al. (2020). The AIR Hurricane Model provides two different 100,000-year catalogs of North Atlantic hurricane activity to represent the risk under (1) all sea surface temperature (SST) conditions as well as (2) under anomalously warm conditions. The latter catalog is referred to as the Warm SST catalog or the WSST catalog, and it was built based on years when the Atlantic Multidecadal Oscillation (AMO) Index has been positive. The warm AMO phase is the one that currently exists, and which has existed since the mid-1990s. More information on the warm SST catalog is available from AIR (2008).

In principle, the large catalog of events also contains events that could occur in a future climate, albeit with a different frequency. The current climate catalogs can therefore be sub-sampled according to a climate change target to create ones that reflect future climate risk. A side benefit of the sub-sampling approach is that because the new catalog consists of different combinations of existing events, the losses by event and other hazard characteristics of the event are already known. Sea level rise is also accounted for in this study in terms of its impacts on storm surge, although resampling cannot create the desired result, so new storm surge footprints for existing events have to be created and the losses to property calculated separately.

Climate change information consistent with an extreme climate scenario is used to define the climate change target. The Representative Concentration Pathway 8.5 (RCP 8.5) scenario is the most extreme of the family of four introduced by the Intergovernmental Panel on Climate Change (IPCC), but several reasons make it an appropriate choice for guidance in this study. One reason is that because none of the RCP scenarios are forecasts, there cannot be any probability associated with any of them, and in that sense, they are all plausible. A second reason is that as an extreme climate scenario it is a good test of the tail of the climate risk distribution. A third reason is that some recent publications (Schwalm 2020) have suggested we have been most closely tracking along the RCP 8.5 scenario in terms of emissions over the last 15 years and that it is a likely scenario for the next 30 years.

Section 8.2 describes the specific methodology for creating the climate change conditioned catalogs from both a wind and storm surge standpoint. Section 8.3 presents hazard and loss results to show the impact of climate change from several different perspectives on wind and storm surge loss. Section 8.4 provides a discussion as well as some next steps to take from a research perspective.

8.2 Methodology

The overall approach involves creating a set of stochastic catalogs of hurricane events to account for the impacts of climate change including SLR. Two different methodologies are employed to account for the climate change impacts on wind and storm surge. Climate change impacts to precipitation are not accounted for explicitly except to the extent that stronger storms tend to have higher precipitation rates (Lonfat et al. 2004).

8.2.1 Accounting for Climate Change Impacts to Wind and Storm Surge

To address wind, the basic approach involves sub-sampling the existing AIR Worldwide U.S. Hurricane 100,000-year WSST catalog of events that reflects the risk in the current climate. The sub-sampling is done in such a way so that the new catalog reflects the potential risk from future climate change. The end result is referred to as a climate change conditioned catalog. A significant benefit of the sub-sampling approach is that the events comprising the climate change catalogs already exist and already have losses computed. Thus, once the climate change catalog is created, the impact on losses is known instantly. This benefit allows many different versions of such catalogs to be created and evaluated very quickly. Each event in the catalog is defined in terms of a maximum windspeed footprint, a maximum storm surge inundation height footprint, and precipitation-induced inland flood depths for on- and off-plain locations.

A prerequisite for creating a climate change conditioned catalog is defining a climate change target to guide the sub-sampling. This target is typically a set of criteria used for deciding whether a randomly drawn event from the parent catalog should be kept or not. The target is typically informed by available information either from peer-reviewed literature, in-house analyses, or otherwise expert judgement. In some instances, to some degree, the target can have some subjectivity associated with it given the fact that the science of climate change and its impacts on complicated weather phenomena is incomplete. In that sense, the target can effectively define a climate change scenario – e.g., how would losses change if the following were to occur. . .

The sub-sampling approach has been used in the past by AIR on a variety of AIR client and industry sponsored projects (e.g., Robinson et al. 2017). The methodology works well, especially when the parent catalog that is being sampled contains a very large inventory of events and when the climate change target does not require events of intensity or landfall location that are not contained in the parent. The more extreme the climate change target is, the less representative the subsampled catalog may be in terms of reflecting expected intensities and frequencies because of the emissions scenario in combination with the time horizon (e.g., RCP 8.5 for 2090).

However, by virtue of using a 100,000-year catalog that represents the current climate to create 10,000-year climate change catalogs that represent the future climate, it is likely that many "new" events that are not in the current climate catalog will appear in the future climate one. The following sub-sections lay the groundwork for creating the climate change target used in this study and how the sub-sampling was actually performed.

8.2.2 Accounting for Changes in Storm Activity

The climate change target for storm activity was created by considering much of the available literature. A recent article by Knutson et al. (2020), and the supplemental material contained therein, was particularly useful for identifying many studies and the wide range of results of how climate change may impact both weak and strong storms. In searching for relevant studies, one challenge was that few, if any, of the studies really show the climate change impacts on an extreme climate scenario (e.g., RCP 8.5) for mid-century. Most studies focus on either an RCP 8.5 or an RCP 4.5 scenario for late century. However, given the known sensitivity of tropical cyclone activity on sea surface temperatures (Evans 1993), it is reasonable to consider how future activity may change according to global temperature increases rather than to RCP scenarios for select time-horizons. To that end, we note that projected increases in global temperature for 2050 under an RCP 8.5 climate scenario are very similar to those for late century under an RCP 4.5 scenario, which is approximately two degrees Celsius (IPCC 2013). Using this equivalence thus allows for some studies to be relevant for defining our climate change target. We present a subset below.

Camargo (2013) examined output from eight different CMIP5 models and found no statistically significant difference between current and future end-of-century climate for RCP 4.5, although the study noted that the coarse resolution likely was a factor, especially in reproducing current tropical cyclone climatology. Knutson et al. (2013) used high resolution numerical downscaling of CMIP5 output to show that category 4/5 storm frequency would increase over the North Atlantic by 39% by the end of the century under an RCP 4.5 climate scenario. The study also showed an overall decrease in storm frequency of 28% that would occur primarily because of decreases in weaker storms. The methodology was applied globally in a later study (Knutson et al. 2015) to show similar results for other basins. Bacmeister et al. (2018) used the Community Atmospheric Model with a horizontal resolution of 28 km and found that under RCP 4.5 for late century, overall tropical cyclone activity decreases over the North Atlantic, but that Category 4/5 storm activity doubles. Roberts et al. (2020) used the CMIP6 HighResMIP Multi-model Ensemble to examine changes in tropical cyclone activity assuming an RCP 8.5 scenario valid for early to mid twenty-first century (2020–2050) relative to mid to late twentieth century (1950–1980) and found no significant changes in tropical cyclone activity. Emanuel (2021) downscaled CMIP6 model output using CHIPs (Emanuel et al. 2004) and showed that major hurricane frequency would increase by 26% and

overall hurricane frequency would increase by 17% for a doubling of atmospheric CO_2, which, according to the IPCC (2013), would occur by mid-century under an RCP 8.5 scenario. Although the result was a global average, the study noted even more significant changes for the North Atlantic.

The considerable spread of results for changes in the frequency of strong hurricanes and overall is summarized in Knutson et al. (2020). We therefore consider the study by Knutson et al. (2013) as a moderate result and as a guide to define changes in the frequencies of strong hurricanes. Table 8.4 from that study was useful for guidance to increase the frequency of major category storms. But it was not followed category by category. Changes in the frequency of weaker storms, even qualitatively in terms of increases or decreases, are less certain as we have noted in our brief review above. To add to the uncertainty, a study by Lee et al. (2020) notes that the overall number of storms projected for the future depends critically on which moisture variable is used in the Genesis Potential Index. Because of the uncertainty, especially about whether weak storms will increase or decrease, we choose for this study to leave the frequencies of category 0–2 storms unchanged. Previous studies have shown that U.S. hurricane losses are dominated by damage from major hurricanes (e.g., Pielke et al. 2008). For stronger, category 3–5 storms, we use the information from Knutson et al. (2013) as well as from the other abovementioned studies as a guide, and define increases of 15%, 25%, and 35% for category 3, 4, and 5 storms respectively. Thus, while the defined frequency target does not necessarily reflect the results from any one study or even in terms of the consensus, it is certainly within the interquartile spread of uncertainty for results that correspond to an RCP 4.5 late-century climate scenario as shown by Knutson et al. (2020), which we note is equivalent to that of an RCP 8.5 mid-century climate scenario. It is also worth noting that by virtue of increasing the frequency of category 3, 4, and 5 storms that the average intensity is implicitly increased. The results of the frequency adjustments by Saffir Simpson category are shown in Fig. 8.1.

Other possible impacts on hurricane activity were considered as part of the target definition, but ultimately excluded. Despite some recent studies that have shown a decrease in forward speed (e.g., Kossin 2018), especially post-landfall, and a poleward migration of the latitude of lifetime maximum intensity (Kossin et al. 2014), Knutson et al. (2019) indicated there is low confidence that they are the result of climate change, and Knutson et al. (2020) expressed low confidence that such trends would continue in the future.

Despite the end result being guided by relevant peer-reviewed literature, and because we will not be considering changes in other storm characteristics like storm size or rainfall rates (as we describe shortly), it is more appropriate to interpret our climate change target as one representing an extreme mid-century climate change scenario rather than an RCP 8.5 climate change scenario.

Sub-sampling was conducted from a landfall perspective, which implicitly makes the assumption that changes in basin activity are the same at landfall. Ting et al. (2019) do suggest that the relatively high vertical wind shear along the U.S. coast that has existed in the past during positive phases of the Atlantic Multidecadal Oscillation, which helps reduce intensities and acts as a protective barrier, may be

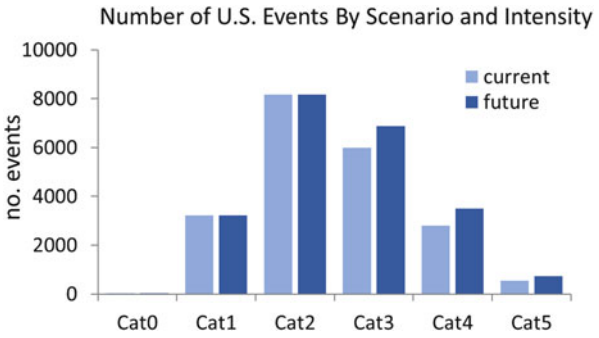

Fig. 8.1 Climate change (future) target frequencies for events by Saffir Simpson Category (by central pressure) at landfall in the U.S. Frequencies for current climate shown for perspective

less effective because of climate change. Thus, the landfall percent increases of intense storms could be larger than those over the basin, although quantifying the result at this point has high uncertainty. The entire catalog of events was partitioned into different Saffir-Simpson categories so that Bin ι contained only storms that made landfall as a category ι storm ($\iota = 0, 1, \ldots 5$). Adjusted frequency targets were created for each category, and then events were drawn at random until the frequency targets for all categories were met.

Many catalogs were created based on the climate change target. The primary reason is because sub-sampling by its very nature begins with a random seed, and because the target is not specified uniquely, a 30% increase in category 4 storms (for example) can be achieved in many different ways. Each catalog that is created meets the target but will differ slightly in other ways. The corresponding industry loss will also be slightly different. And, for any one catalog, the increase of Category 3–5 storms may differ slightly in certain regions from that of the specified target, but for several catalogs together, the target is essentially preserved. We show the sensitivity of this in the next section. Generating one thousand different catalogs provides enough samples so that the spread in losses can be accurately obtained.

8.2.3 Accounting for Sea Level Rise Impacts to Storm Surge

In order to account for the impacts of sea level rise on storm surge, new storm surge footprints for each existing hurricane event in the 100,000-year catalog had to be created regardless of storm intensity. Sub-sampling the existing storm surge footprints was therefore not an option, and a more complex solution and procedure had to be developed and implemented. Losses for these new storm surge footprints were calculated using the loss module of the AIR Hurricane Model.

Storm surge is currently modeled in the AIR Hurricane Model using a form of the National Oceanic and Atmospheric Administration (NOAA) Sea, Lake, and Overland Surges from Hurricanes (SLOSH) Model (Jelenianski et al. 1992). The AIR SLOSH model accounts for hurricane parameters, coastal geography, coastline features, tidal rivers, and flood defenses, but uses AIR Hurricane Modeled winds

from a stochastic catalog of events. Tidal effects are included by computing a tidal height for each event, considering the simulated landfall date and time, the landfall location, and other adjustments based on the local geography and seasonality. The raw surge elevation output is then post-processed using a high-resolution 30 m digital terrain model to calculate storm surge depths at a 30 m resolution. Damage to property and contents is computed using that information along with AIR-developed damage functions that are appropriate for the building and contents within.

The AIR 100,000-year U.S. Hurricane catalogs each contain over 200,000 storm surge events. Resimulating these for different sea level rise scenarios is computationally expensive and time consuming. An alternate technique was therefore developed that allows the current climate storm surge footprint to be spread across a future climate land-seascape with the prescribed amount of SLR. The technique begins by increasing the storm surge heights at all land cells that are wet and all water cells by the prescribed amount of SLR. A series of sweeps is then performed to determine which additional cells will get wet. With no underlying friction present, a dry cell is wetted to an average surge height based on the average of the surge heights from the surrounding wet cells. If the average surge height is higher than the elevation of the grid cell in question, then the cell remains wet with the average surge height elevation. Without friction, the inland extent of the new surge footprint is limited by the distribution of terrain height. The methodology is explained in more detail in McInnes et al. (2013). This strategy allows for new storm surge events to appear in the catalog to the extent the base (e.g., without SLR) storm surge footprint contained some footprint just offshore that could be extended inland.

In this study, to improve upon this terrain-height-limited footprint, friction is introduced to allow a more realistic inland penetration of storm surge. The friction is parameterized according to the land-use of the underlying surface. A single value is used here for all cells that favors urban areas near the coast that would typically exhibit the most damage from storm surge. The value is chosen based on a limited set of calibration runs with SLOSH. We note that the approach used here does not capture the change in dynamics that sea level rise may have on storm surge, which on very local scales can be significant. These effects have been studied by numerous authors (Lin et al. 2012; Zhang et al. 2013; Bilskie et al. 2016), and although nonlinearities do exist as a function of bathymetry, land slope and friction, storm characteristics, etc., the general finding is that the impact of SLR produces a linear addition to the height of the water. Once the footprints are adjusted for SLR, the output has to be reformatted in order for the files to run within the loss estimation module in AIR's Touchstone® Software. This requires almost as much processing time as the SLR adjustment phase. Thus, only three regions of the U.S. are processed for this study: Galveston-Houston, Miami, and New York City.

8.2.4 *Regional Sea Level Rise Projections*

Regional projections of SLR are obtained from Sweet et al. (2017). This source provides very detailed information for a variety of scenarios that incorporate different RCP information and more. Additionally, there is an accompanying user-interactive web site that allows scenarios to be obtained for a large number of tide gage stations along the U.S. coastline. Typically, six different scenarios are shown for every station and are labeled as Low, Intermediate-Low, Intermediate, Intermediate-High, High, and Extreme. Figure 8.2 shows the global mean sea level rise version and the correspondences to the RCP scenarios.

Because of our focus on mid-century, the values in 2050 are relevant. Additionally, to capture some of the uncertainty of sea level rise within the RCP 8.5 scenario, we choose the Intermediate-Low and Intermediate-High scenarios, which are the two that most closely flank the 5–95% certainty boxes in Fig. 8.2. Increases were determined from 2010, which is the vintage of the bathymetry and elevation data in the AIR hurricane model. An example of how the values was determined for the Intermediate-High scenario for New York is shown in the bottom panel of Fig. 8.3. The values for both SLR scenarios for each region are shown in Table 8.1.

These SLR amounts were used in the adjustment process for all storm surge events that affected each of the three regions (The regions are shown in Figs. 8.10, 8.15, and 8.20). For example, for all events affecting Galveston, 14.2 inches and 25.6 inches were used in the storm surge adjustment process described above.

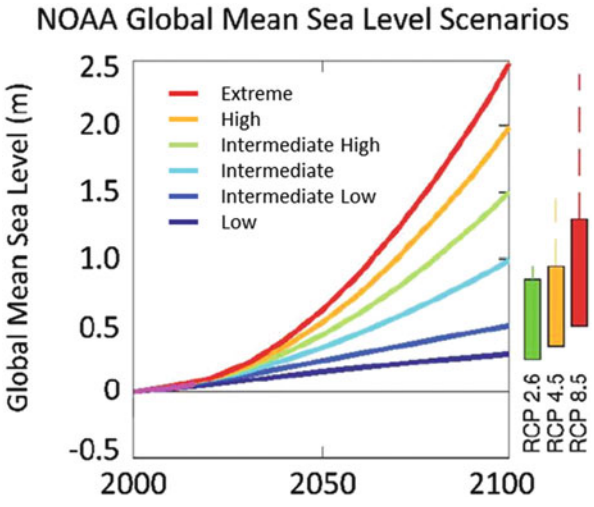

Fig. 8.2 Six representative Global Mean Sea Level rise scenarios for 2100 (six colored lines) relative to historical reconstructions from 1800–2015 and central 90% conditional probability ranges (colored boxes) of RCP-based Global Mean Sea Level Rise projections. Central 90% probability ranges augmented (dashed lines) by difference between median Antarctic contribution of Kopp et al. (2014) probabilistic GMSL/RSL study and the median Antarctic projections of DeConto and Pollard (2016), which have not yet been incorporated into a probabilistic assessment of future Global Mean Sea Level Rise scenarios. (Adapted from Sweet et al. 2017)

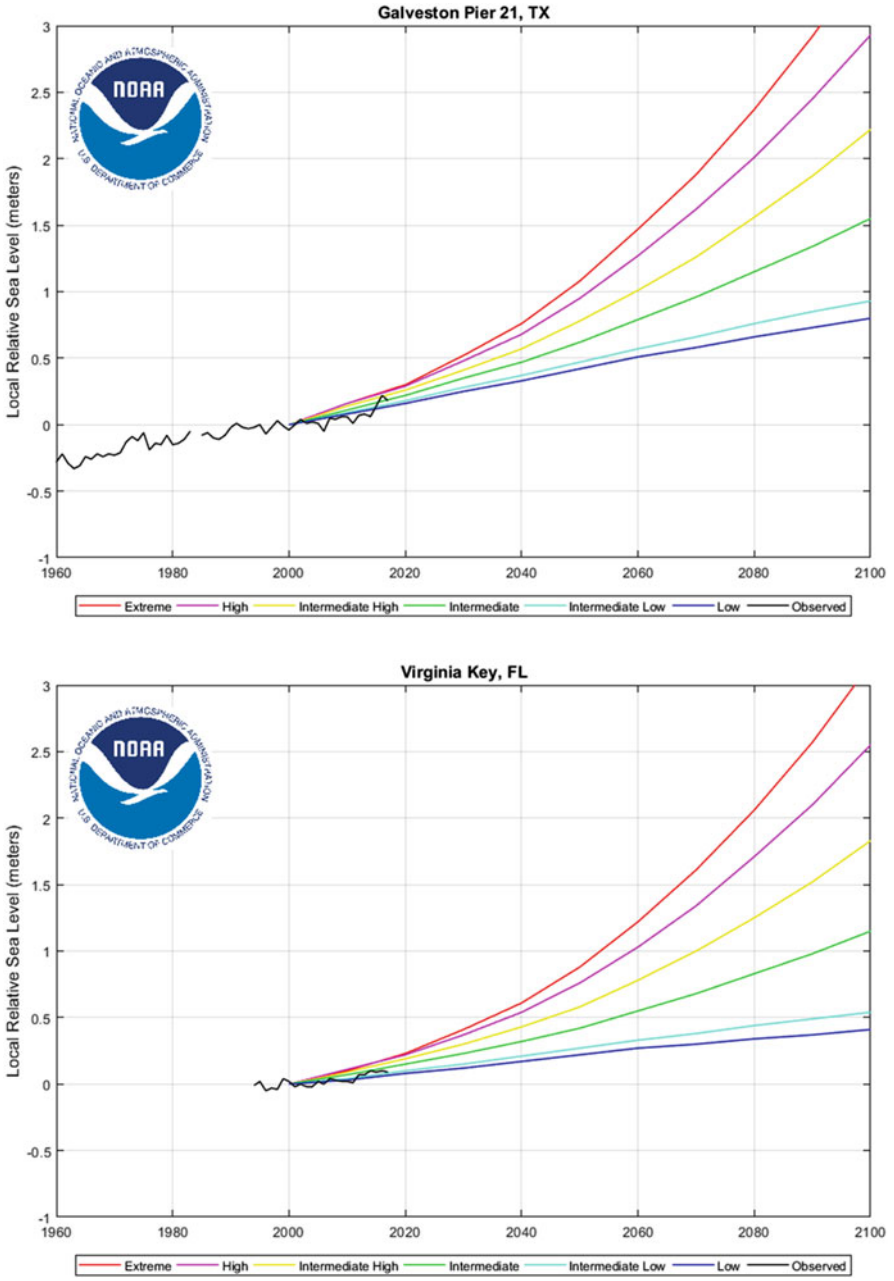

Fig. 8.3 NOAA SLR scenarios for locations used in the study. Annotations in bottom panel indicate considerations for adjusting the SLR value needed for 2050 for one NOAA scenario (yellow, intermediate high) because of the vintage (2010) of the storm surge output from the SLOSH model. More details provided in the text. (Plots obtained from NOAA website: Sea Level Trends – NOAA Tides & Currents)

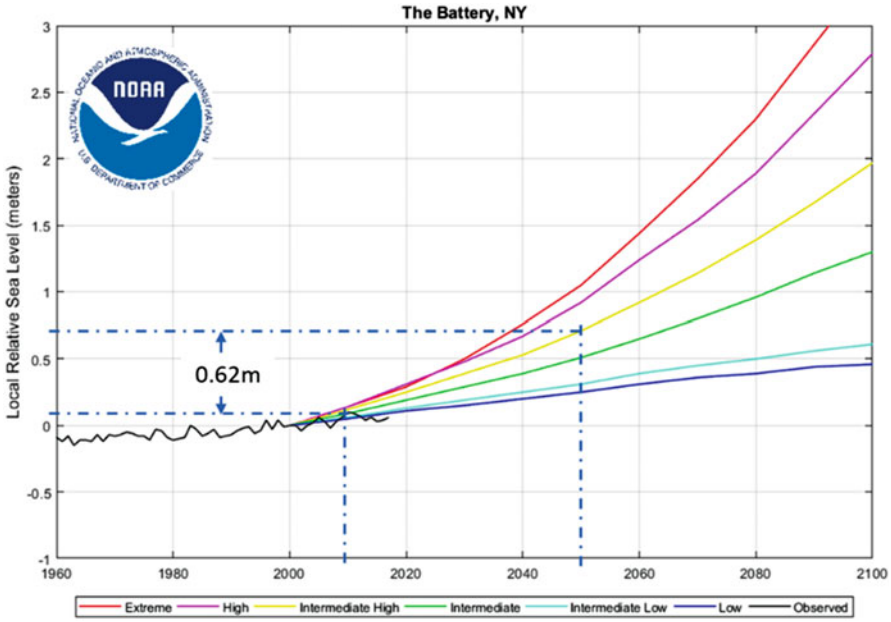

Fig. 8.3 (continued)

Table 8.1 Sea level rise values calculated for use in the three regions of study for the two SLR scenarios chosen

Region (buoy)	Intermediate low (inches)	Intermediate high (inches)
New York, NY (The Battery)	8.3	24.4
Miami, FL (Virginia Key)	7.5	20.1
Galveston, TX (Galveston)	14.2	25.6

All stochastic events that generated storm surge along the coastlines and even just offshore of each of the regions, including a 50-nautical-mile wide buffer on either side from the first 50,000 years in the AIR 100,000-year WSST catalog, were identified and evaluated for impacts from sea level rise. This resulted in 8527 events for the New York region, 16,643 events for the Miami region, and 20,173 events for the Galveston region. The number of events that actually cause loss in the counties shown in the three regions depended on the SLR scenario.

8.3 Results

We describe here some hazard and loss results at the national and county levels before focusing in more detail on the three urban regions. More detail for the national and county level results is presented in Grenier et al. (2020).

8.3.1 *Regional Distribution of Landfall Activity*

The subsampling of the AIR U.S. hurricane catalog to create a frequency/intensity distribution reflective of our mid-century extreme climate scenario yields a 20% net increase in major hurricanes making landfall. Because there was no further constraint on activity – e.g., regional changes – the 20% increase occurred more or less uniformly over the entire coastline affected by hurricane activity, but only when multiple 10,000-year catalogs of activity are considered. Figure 8.4 shows the

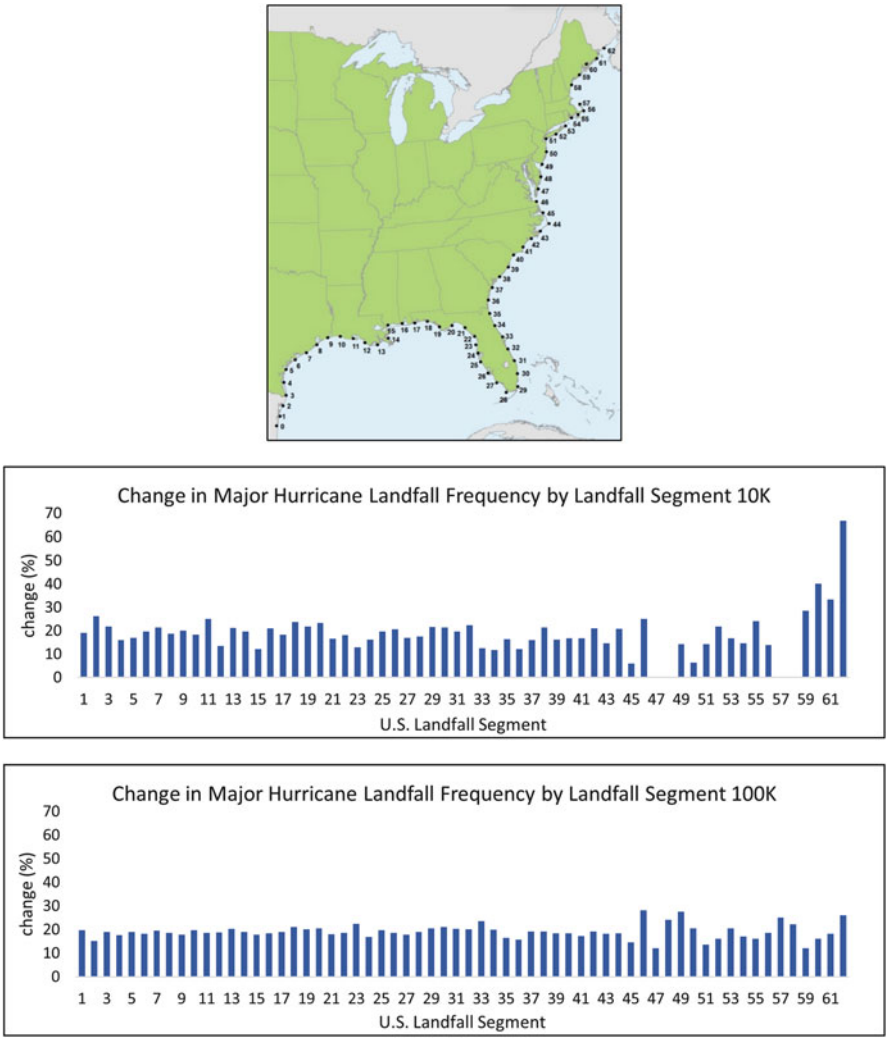

Fig. 8.4 Landfall segments used in the AIR U.S. Hurricane Model (upper panel) and percent changes in landfall frequency of major hurricanes by segment from a 10 K climate change catalog (middle panel) and from a 100 K climate change catalog (lower panel) relative to current climate

geographical landfall distribution of major hurricanes from a single 10,000-year (10 K) catalog and from the aggregate activity of 10 such catalogs together (e.g., effectively 100,000 years of activity). Clearly, there are more accentuated regional differences indicated by the 10 K view, but it is important to note that they are spurious and that there is no physical reason to explain it. The variations by coastline segment are a result of the openly defined target used to create the catalog.[1] Even with the 100 K catalog, the distribution by landfall segment is not perfectly uniform. Segment 47, for example, shows an increase of only 12%, although it is shouldered on either side by 28% and 24% increases. As a larger region, segments 45–49 together yield an average increase of ~21%. The non-uniformity for this region, even from a 100 K catalog, is related to the relatively low landfall rate, which is a result of the NW-SE oriented coastline at a latitude where storms are typically recurving away (e.g., NE-ward) from the coast.

8.3.2 National Loss Results

Impacts on loss from each of the climate change catalogs were evaluated at national, state, and county levels. One big advantage of the sub-sampling strategy is that because the events that go into the sub-sampled catalogs have already been run through the AIR Hurricane Model loss module, the information about where and how much loss, as well as further granularity of loss to particular lines of business (e.g., residential property, commercial property, automobiles, etc.), is already known. That is a great advantage because processing even one 10 K catalog to generate losses is computationally expensive. The loss estimates here consider the direct damage to exposures, such as residential, commercial, and industrial properties, and automobiles, etc., and the temporary loss of use of those exposures caused by that damage. The AIR Industry Exposure Database has been developed using data obtained from a variety of data sources, including private vendors, government reports and databases, and remotely sensed information. It includes the primary building material (wood, steel, concrete), use type (residential, commercial, industrial), number of stories, year built, etc., and replacement cost, all of which impact building vulnerability, damage, and loss. The database reflects all insurable property on a 90 m grid for the entire U.S. It does not include non-modeled exposures such as public infrastructure, marine, or cargo, or indirect sources of loss, such as lost wages or economic productivity. More information on the AIR industry exposure database is available from Hayes and Rowe (2008).

Loss metrics typically involve an average annual loss, an average occurrence loss, and return period losses, either from an occurrence or aggregate standpoint and from an insurable or insured standpoint. Average Annual Loss (AAL) is the average loss

[1] It is important to note that variation from one 10 K catalog to another in this respect is not an indication of the lack of convergence in the 10 K catalogs that are provided to clients because of other calibration measures that are implemented.

across all years in a stochastic catalog, or the expected loss per year averaged over many years. Average Occurrence Loss (AOL) is the average of the largest annual single event losses. Return period losses represent the magnitudes of loss at different exceedance probabilities. A 10,000-year loss in the 10,000-year catalog is the largest loss in the catalog. The 5000-year loss is the second largest and so on. Equivalently, a 5000-year loss can be referred to as having a 5000-year return period or a 0.02% exceedance probability. Again, this can be either from an aggregate (all event losses in a year summed) or from an occurrence (single largest loss in a year) standpoint. Insurable losses are based on the fraction of damage/loss relative to the total replacement value. Insured losses account for deductibles, limits, etc. that characterize the exposure in question. The AIR Industry Exposure Database uses location-averaged information for deductibles, etc. Clients who use the AIR software to compute their own losses can enter more specific information about buildings, contents, and policies.

The impact to losses for the entire U.S. is summarized in Fig. 8.5. Specifically, the distributions in AAL, 100-year return period aggregate loss, and 250-year return period aggregate loss from the 1000 different 10 K climate change catalogs are shown relative to the distribution of losses from the 1000 different 10 K catalogs that were sub-sampled to represent the current climate. To a large degree, the 20% fingerprint from changes in frequency of major hurricanes (storm activity) is evident in the AAL. The median loss change for the AAL is 19%. The agreement is more than coincidental because the result demonstrates that the bulk of the damage to U.S. property occurs by far and away from major hurricanes. The slightly larger spread in losses for the future climate is a reflection again of the open-ness of the target used for sub-sampling, the heterogeneity of the exposure and its vulnerability across the U.S., and the regional landfall frequency, particularly of major hurricanes, even for the current climate. It is important to note that the spread in losses is the result of the sampling variability associated with achieving the climate change target, not a reflection of the scientific uncertainty associated with the climate change impact. To that end, it is notable that the spread in loss results for the two return periods (both show median changes of ~15%) is notably larger than that for the AAL for both the current climate and the future climate. Again, this reflects the openness of the target and the heterogeneity of the exposure distribution across the U.S.

The percent changes by sub-peril (not shown) are also comparable given that the sub-sampling target did not specify any constraints on precipitation or storm surge. The 20% increase in flood AAL is more related to the net increase in storm activity and is much less sensitive to stronger hurricanes generating more precipitation. For precipitation and inland flood, it is reasonable to expect that because of the Clausius-Clapeyron effect, and all else equal, that precipitation and possibly flood would increase by about another 7% (given the assumed additional one-degree Celsius increase that would occur by 2050 under RCP 8.5). Storm surge would also increase more across the entire U.S. hurricane-affected coastline because of sea level rise, an aspect we evaluate later in this section in more detail for select locations.

It is important to note that the loss results in Fig. 8.5 reflect the direct damage to the full database of exposure (i.e., insurable), not just the insured portion. The insured portion would be significantly lower particularly for the surge and flooding components, which are significantly underinsured.

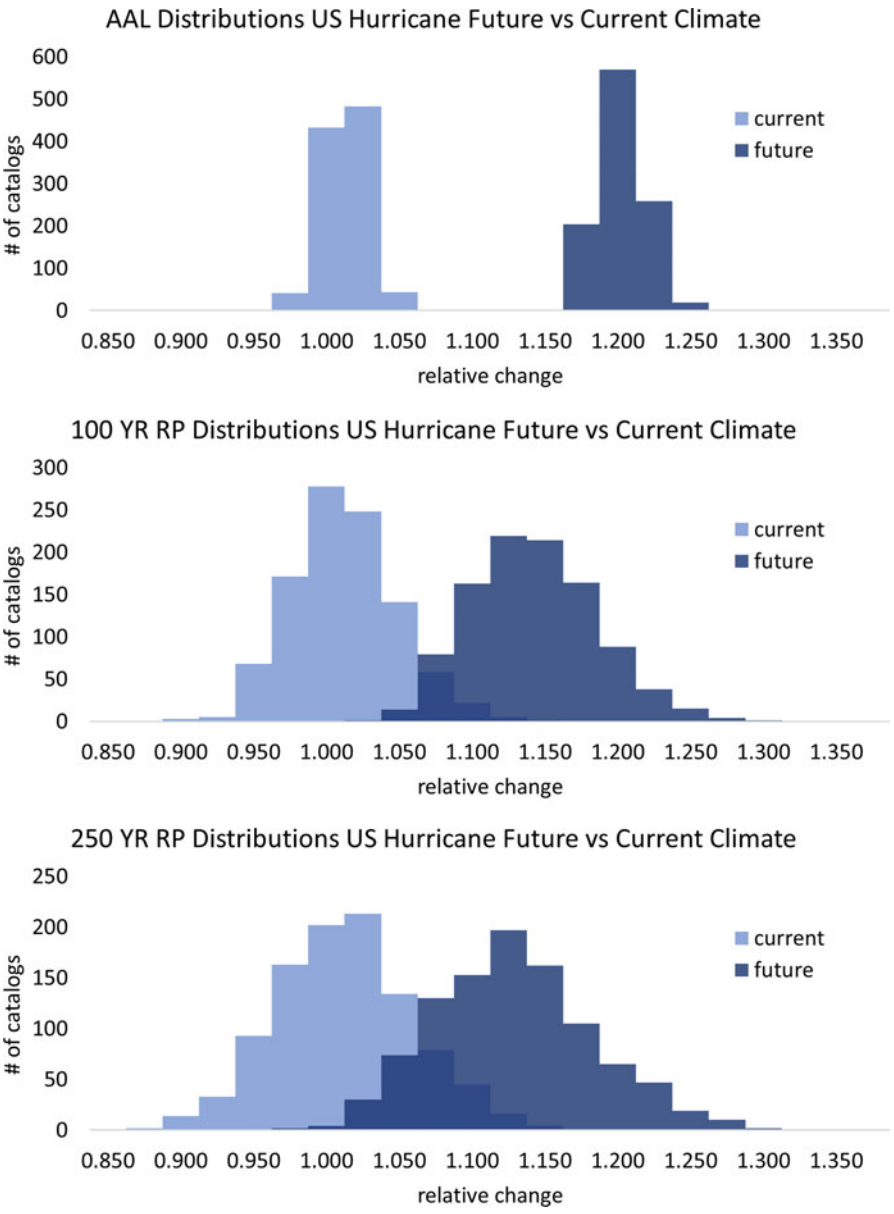

Fig. 8.5 Distribution of aggregate insurable loss changes for future climate catalogs relative to current climate. Spread is result of each catalog yielding a slightly different loss. Current climate catalogs are generated in a way similar to future ones to provide a better basis for comparison. Losses normalized by mean value of current climate loss

8.3.3 County Level Loss Changes

Additional insight into the geographical changes in hurricane risk for the climate change scenario as we have defined it is gained by considering loss results by county. Figure 8.6 presents county level detail of the AAL for current and future climate and for the change in AAL for all sub-perils combined. At first glance, there appears to be little difference in the distribution of current and future climate losses, and to a large degree this is likely attributable to the absence of any regional differences in landfall activity as shown in Fig. 8.5 (bottom panel). However, a view of the percentage difference plot in Fig. 8.6 does show coherent structure. The spread of percentages is admittedly small, as might be expected, but given the numbers of events involved in the calculations, the differences are statistically significant. One curious feature is that the highest percent changes are not exactly right along the coastline everywhere as might be expected. In fact, the only coastal area where changes are highest is in Florida across the eastern two thirds of the peninsula. A discontinuous band of highest percentage loss increase exists 100–500 km inland stretching from east Texas, eastward to Alabama then northeastward to southern North Carolina. Lower percentage changes exist farther northeast, with the smallest percentage increases over the central Appalachian region.

Some insight to this pattern can be obtained from Fig. 8.7, which shows the relative changes by sub-peril. Percent changes for wind and inland flood losses are even farther inland, while those for storm surge are adjacent to the coast. The distribution of sub-peril relative loss changes for wind and inland flood are likely a combined result of distribution of the hazard changes, damage function dependence on wind speed and flood depth respectively, and distribution of exposure. The second point is worth explaining more. Damage functions for windspeed typically are nonlinear, given that the force and power of the wind increase as the square and cube of the windspeed respectively, but even more so because at some high windspeed value, building fixtures, including parts of roofs, overhangs, exterior lamps, etc., tear off and become projectiles, which can cause even more damage by breaking windows of other buildings, thus breaching other building envelopes so that wind and water can enter those structures and cause even more damage (the AIR damage functions account for such effects). The fact that the highest percent increases in wind loss are slightly inland may reflect the nonlinearity of wind damage to wind speed – specifically, it is the zone where the change in storm activity creates the greatest impact from a fractional building damage perspective.

For flood (both precipitation-induced and coastal), the water typically has to reach a certain depth for a structure to be damaged. The farther inland location of maximum increase in precipitation-induced flood damage in Fig. 8.7 (middle panel) may be the result of more storms generating flood water that affects a greater number of properties annually on average, plus the fact that heavy precipitation typically extends much farther inland even as tropical cyclone winds decay below property-damaging strength. The distribution of changes in storm surge loss is easier to interpret, with a near continuous band of change along the coast and with some

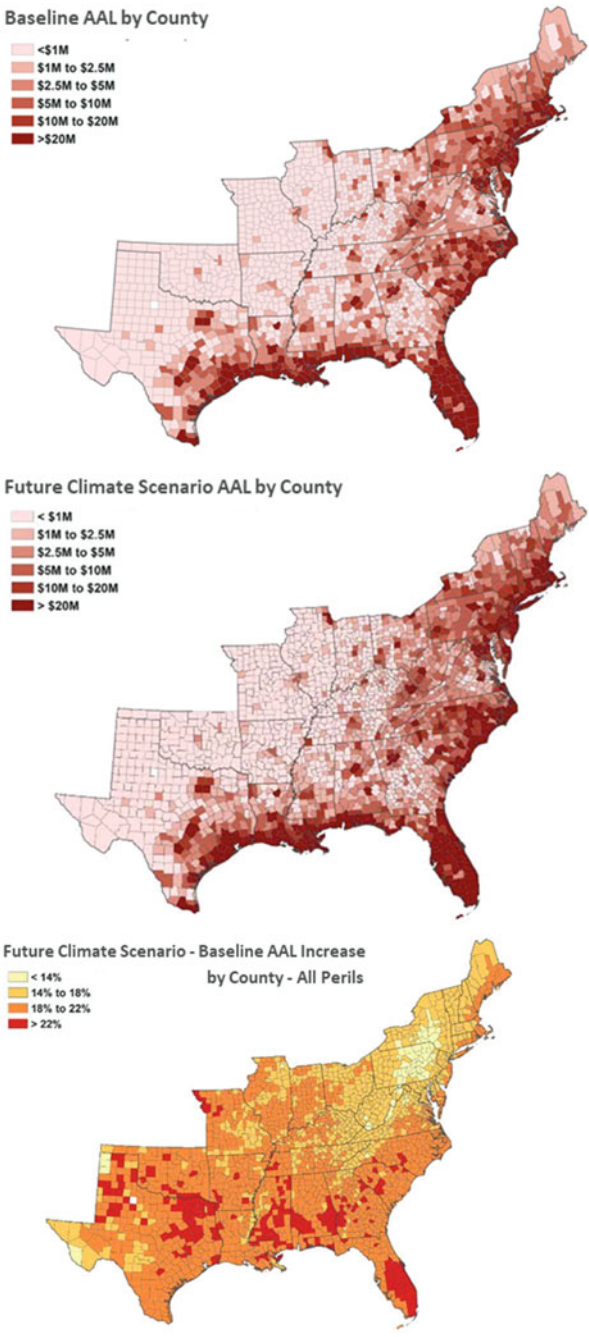

Fig. 8.6 Average annual loss (all sub-perils) for current climate (upper), future climate (middle), and percent change (lower). Note: changes for all sub-perils are from change in hurricane frequencies by Saffir Simpson Category only

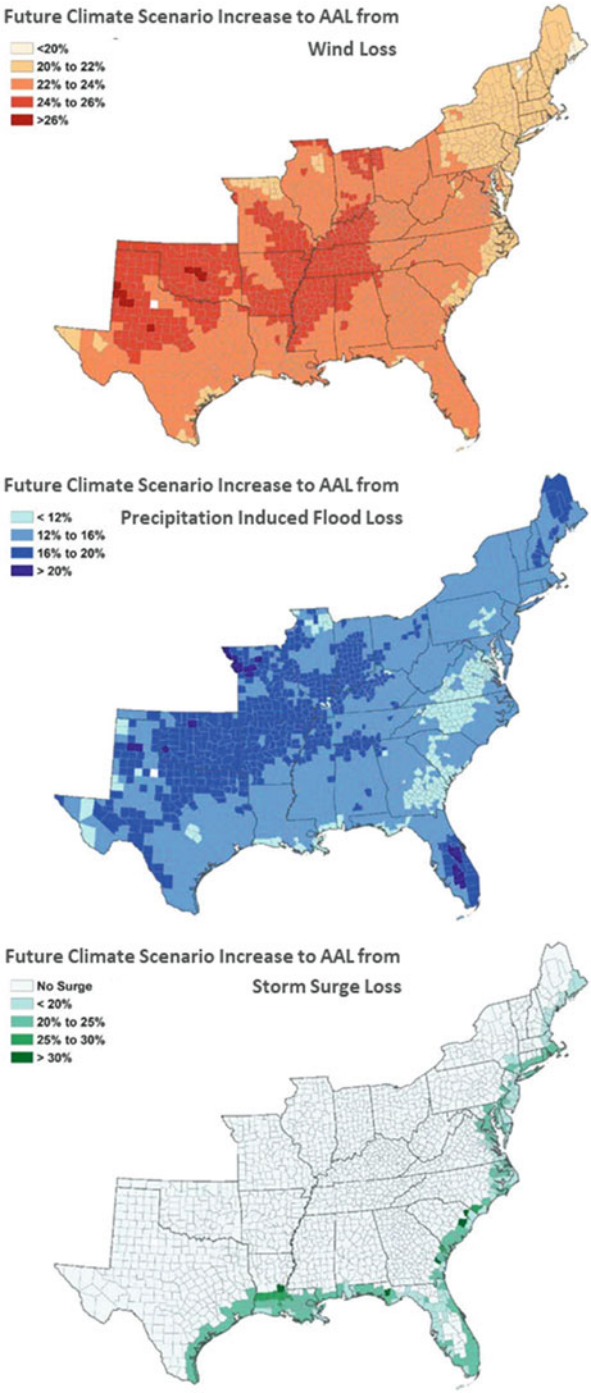

Fig. 8.7 Relative changes to AAL from sub-peril losses as shown. Note: changes for all sub-perils are from change in hurricane frequencies by Saffir Simpson Category only

innermost locations exhibiting the highest change. This last feature is likely a result of areas experiencing storm surge damage from additional strong storm activity in the future climate that do not in the current climate.

The slightly lower percent increases in loss over the mid-Atlantic region extending northward appear to be driven more from wind loss rather than from precipitation-induced flood loss. Even though this region still experiences a 20% increase in major hurricanes, it is almost certainly the case that on the whole the storm intensities are weaker than those impacting the southern U.S. and that storms decay faster inland (because of mountainous terrain), and thus likely that fewer properties experience damage consistent with a 20% increase in major storm activity. This explanation is consistent with the fact that increases in storm surge loss for the U.S. coastline from Virginia northward are basically the same as for locations farther south, especially for coastlines oriented perpendicular to storms approaching from a southern direction.

8.3.4 Detailed Loss Analyses for Selected Urban Locations

The results in the previous sub-section showed potential climate change impacts to storm surge loss from increases in storm frequency (i.e., Fig. 8.7 bottom panel). Impacts from SLR were not included for that analysis because the methodology described in Sect. 8.2 to adjust storm surge footprints for SLR is still computationally involved – especially because hundreds of thousands of events need to be processed. Thus, for this study, we focus on three regions where relative impacts to storm surge loss from changes in storm activity and sea level rise are compared, and storm surge loss relative to wind loss is also compared. The three regions are Houston, TX; Miami, FL, and New York City, NY, and the counties included are shown in Fig. 8.8. Despite spanning less than ten percent of the coastline impacted by hurricane activity, these three regions alone account for approximately one-third of the AAL from U.S. hurricane activity.

For some additional background information, we show in Fig. 8.9 the contribution of storm surge loss to wind and surge AAL by Saffir Simpson category from the AIR Hurricane Model. The result for the entire coastline (see Fig. 8.4 for segments) is shown (i.e., segments 1–63), as well as for several subregions of coastline including the Gulf Coast (segments 1–17), Florida Coast (segments 18–35), southeast U.S. coast (segments 36–44), and the northeast U.S. coast (segments 45–63). In all cases, the relative contribution decreases with increasing hurricane intensity. Although there is little information in the literature on the topic, this result may be understood in part by realizing that the wind damage functions are very nonlinear in terms of fractional damage with respect to wind speed, and that storm surge damage functions tend to be more linear with respect to water depth (Sealya and Strobl 2017; USACE 2020). Additionally, even though storm surge height and depth depend non-linearly on wind speed (Harris 1957), wind damage will typically extend farther inland and do more damage with increasing storm strength than storm surge damage

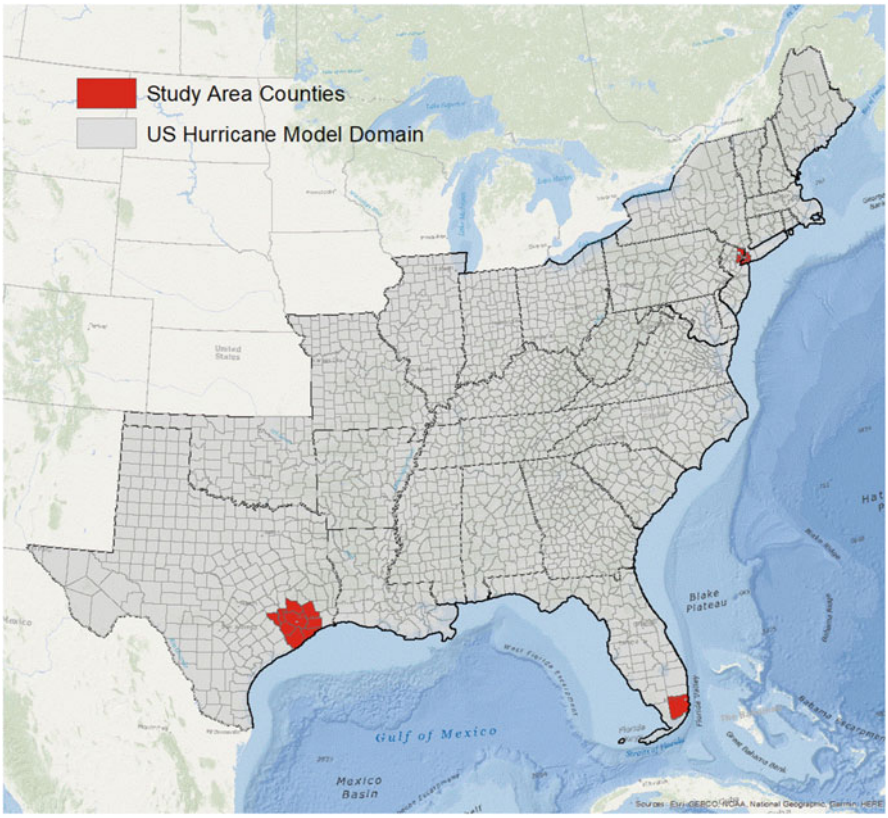

Fig. 8.8 Locations and extents of the three study regions for detailed SLR and storm surge analysis: Metro NYC, Miami-Dade, and Houston/Galveston (regions range from one to nine counties). Shaded states indicate domain of AIR Hurricane Model

can, especially in steep coastal terrain. Specific behavior of wind and surge damage functions depends on a multitude of factors, including building material, building height, flood mitigation, etc., and hence the different behaviors in Fig. 8.9 for the different coastline sections (e.g., convex vs. concave) cannot be completely understood without a more detailed assessment.

8.3.5 Galveston-Houston Return Period Wind and Storm Surge Results

This region is typically impacted by hurricanes. Although Hurricane Harvey in 2017 made landfall well south of Galveston, seventeen storms of category strength one or higher have made landfall within 50 nmi of Galveston since 1900. This frequency is

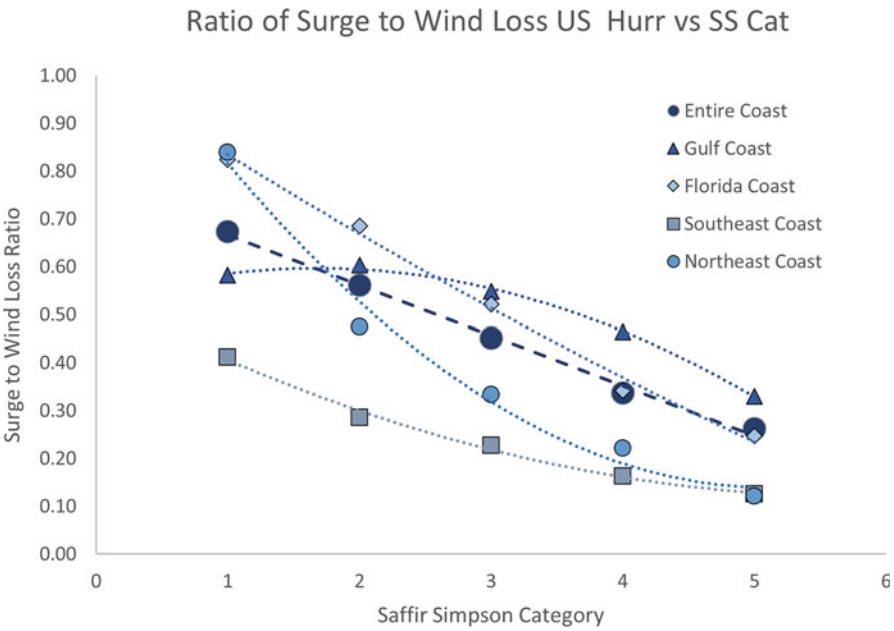

Fig. 8.9 Ratio of storm surge loss to windspeed loss by Saffir Simspn category in the AIR Hurricane Model. Region definitions in terms of landfall segments explained in text. Best-fit curves using second-degee polynomials included for all segments except for Entire Coast which has best fit line

accurately reflected in the current climate of the AIR Hurricane Model. As noted for this study, sub-sampling increases the frequency of major category strength storms by ~20%, and as we have seen, because of those storm changes, wind and surge losses increase by a little over 20%, and inland flood losses increase by a little less than 20%. However, SLR will increase storm surge loss relative to wind loss, and so it is worth looking at how the relative contribution of storm surge to wind and surge loss changes because of SLR. Figure 8.10 shows the contributions for current sea levels by county for reference.

The coastally adjacent counties (Brazoria, Galveston, and Chambers) currently experience relatively high percentages of loss from storm surge. Even Harris County, where downtown Houston is located, shows a 5% contribution because of a short stretch of coastline along the northern lobe of Galveston Bay and because of an adjacent deeper inlet that gets flooded. The inlet is in fact the reason why Liberty County also experiences some coastal flooding. Select return period storm surge inundation maps from the AIR (SLOSH based) storm surge model for the current climate are shown in Fig. 8.11 and provide some additional perspective on areas prone to coastal flooding. Plotted resolution for all return period storm surge maps is roughly 250 m, and each grid cell inundation height (e.g., storm surge height above

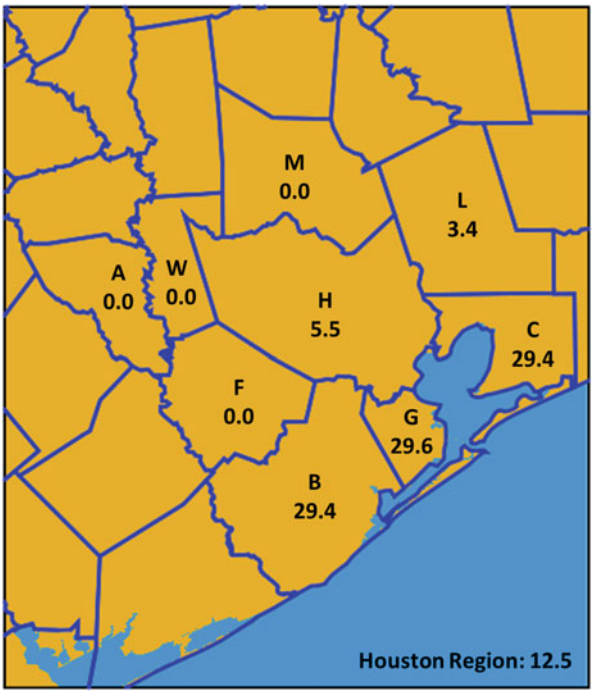

Fig. 8.10 Percent contribution (numbers) of storm surge to wind+surge AAL by county (indicated by first letter) for Austin, Brazoria, Chambers, Fort Bend, Galveston, Harris, Liberty, Montgomery, and Waller Counties for current climate. Nine county average for Houston Region is 12.5%

mean sea level) represents the return period value from all storm surge events impacting that grid cell.

As noted previously, the higher frequency of major hurricanes in our future climate scenario increases the wind and storm surge losses by approximately 20%, and thus the percent contribution of surge to wind and surge loss at the county level is essentially no different than for the current climate result shown in Fig. 8.10, so it is not shown. Sea level rises differentiates the relative contribution from storm surge loss significantly and is explored in more detail. Table 8.2 summarizes the impacts of SLR and increases in storm frequency on storm surge losses. Both SLR scenarios result in significant increases in storm surge loss.

The Intermediate-Low and Intermediate-High SLR scenarios increase storm surge AAL by 41% and 84% respectively. The increases in AAL are primarily attributable to increases in depth of areas that already get inundated without SLR, although some increase in AAL is the result of additional areas getting inundated. The percent breakdown is not calculated here, but some insight can be obtained by examining the storm surge footprints. To that end, storm surge footprints for select RPs for both SLR scenarios, including increases in storm frequency, are shown relative to those for current sea level and frequency conditions (the base case) in Fig. 8.12 to illustrate the point. We note that from Fig. 8.11, for a given RP, a comparison of the inundation areas for the Intermediate-Low and Intermediate-High SLR scenarios shows very little change in area inundated. One has to look carefully

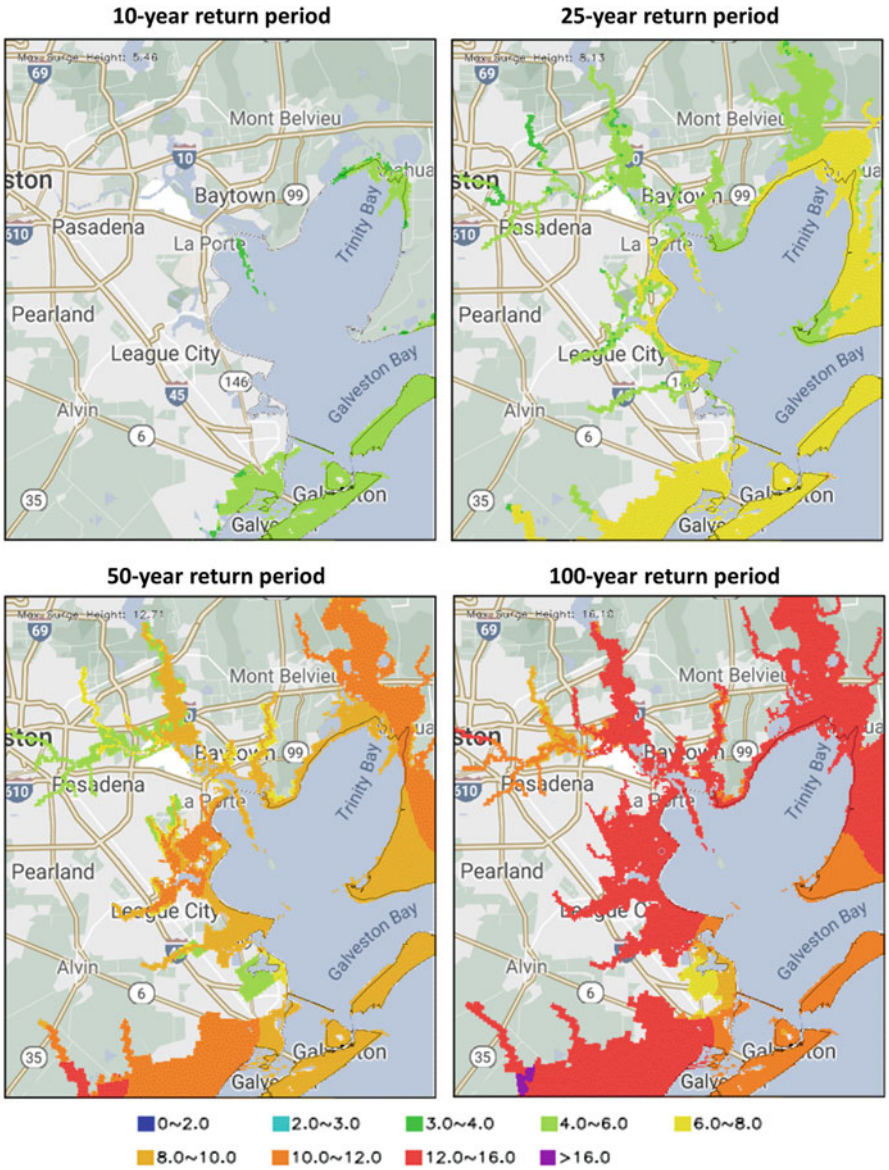

Fig. 8.11 Storm surge inundation height (feet) for Galveston-Houston Region for return periods and current sea levels. Plotted domain spans 0.60° lat × 0.60° lon. Downtown Houston is just outside western edge of plots

to identify signatures. For the 100-year RP, the differences are shown in Fig. 8.13. The contribution to the footprint size from just SLR and from SLR and increased storm frequency is shown. A comparison of the two plots shows that the additional

Table 8.2 Summary of impact of SLR and changes to storm frequency on storm surge loss for Galveston-Houston Region

Scenario	Pct change in surge AAL	Pct contr surge to wind+surge AAL
Current climate	–	12.5
Incr freq	23	12.5
Int-lo SLR scenario	41	16.8
Int-lo SLR scenario + incr freq	72	16.7
Int-hi SLR scenario	84	20.8
Int-hi SLR scenario + incr freq	123	20.6

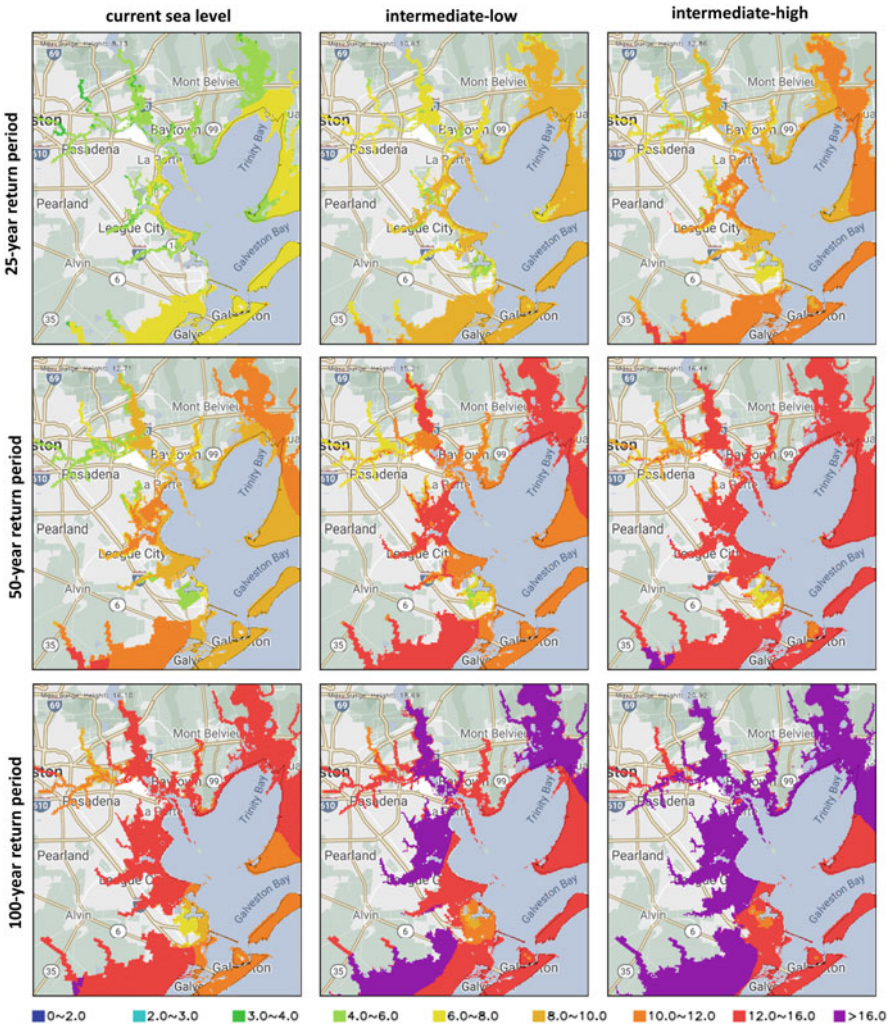

Fig. 8.12 Storm surge inundation heights (feet) for Galveston-Houston Region for return periods and SLR scenarios as shown. Plotted domain spans 0.60° lat × 0.60° lon. Downtown Houston is just outside western edge of plot

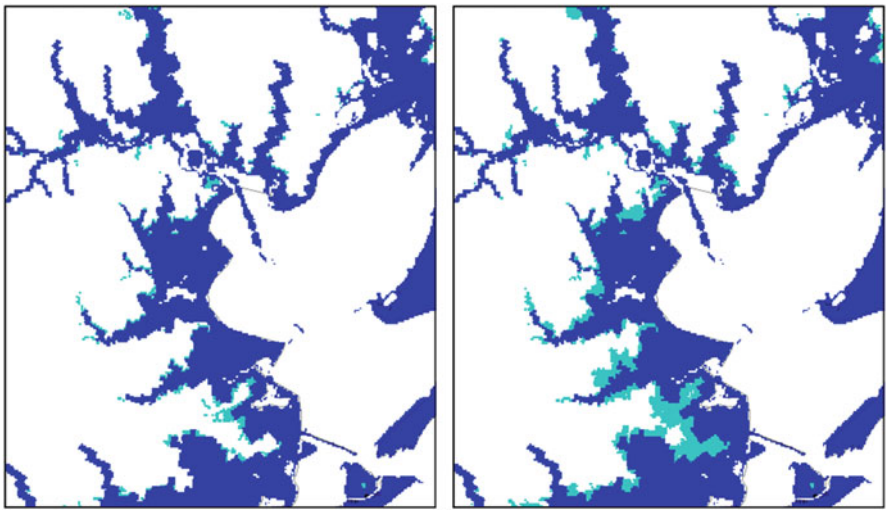

Fig. 8.13 Additional areas inundated (light blue) relative to current sea levels and storm frequency (dark blue) for Intermediate-Hi SLR scenario without frequency increases (left) and for Intermediate-Hi SLR scenario with frequency increases (right) for Galveston-Houston region for 100 year RP. Base map removed for clarity. Plotted domain spans 0.60° lat × 0.60° lon

Table 8.3 Relative contribution to storm surge footprint area for Galveston-Houston region for select return periods (top row in years) and for varous climate scenarios

Scenario	1000	500	250	100	50	25	10	5
Base	62,160	56,979	51,328	42,461	36,255	28,357	8337	0
Int lo w/o freq incr	1.1	0.9	0.7	2.6	2.8	4.4	62.9	–
Int lo w/ freq incr	4.0	3.7	3.2	6.5	7.1	10.4	105.4	–
Int hi w/o freq incr	1.4	1.1	1.0	**3.2**	3.3	5.0	70.9	–
Int hi w/ freq incr	5.1	6.1	6.1	**10.1**	10.8	17.9	145.6	–

Numbers for base indicate the numbr of inundated cells for current conditions. Bold numbers correspond to the changes shown in Fig. 8.14

impact of increased storm frequency combined with SLR is comparable to the impact from SLR alone. Table 8.3 shows a more complete summary in terms of the impacts to other RPs as well as for the Intermediate-Low SLR scenario. The contributions from increased storm frequency combined with SLR are obviously more significant at lower RP values, as whatever protective measures to prevent/inhibit coastal flooding are overcome. The numbers provide some insight into how losses increase because of changes in footprint size vs. increases in depth, but they do not tell the whole story.

In contrast to the small changes in footprint size, inundation heights increase on average by the amount of the SLR over large, already-inundated areas. Table 8.4 illustrates this more clearly. Maximum inundation heights are shown for different combinations of storm frequency and SLR scenarios. Especially for the higher return

Table 8.4 Maximum storm surge inundation heights (feet) for Galveston-Houston region for return periods (left column, years) and climate scenarios as shown

RP	Current SLR		Interm low		Interm high	
	w/o freq incr	w freq incr	w/o freq incr	w freq incr	w/o freq incr	w freq incr
5	0.00	4.32	6.03	5.50	6.03	6.83
10	5.46	5.95	7.59	7.13	7.59	8.53
25	8.13	9.18	10.26	10.63	10.26	12.86
50	12.71	13.54	14.90	15.21	14.90	16.44
100	16.10	17.51	18.38	18.69	18.38	20.92
250	22.61	24.16	24.74	25.34	24.74	27.08
500	26.97	28.57	29.10	29.75	29.10	33.85
1000	33.42	34.90	35.55	36.08	35.55	37.04

Current refers to current storm frequency, future refers to increased frequency for major category storms as descibed in the text

periods, augmentation of the maximum inundation height from a higher frequency of major storm activity is just as significant as the impact from SLR alone. For example, the 100-year RP maximum inundation height for the Intermediate-High SLR scenario is 2.28 feet higher than for the current SLR scenario without an increase in storm frequency. The inclusion of additional storm activity to the Intermediate-High SLR scenario adds another 2.54 feet to that maximum (although not necessarily in the same place).

A side note to the RP inundation footprints shown in Fig. 8.12 is the linear nature of the response (e.g., the maximum inundation height increases by the amount of SLR). A range of published literature shows the impact of SLR on storm surge in general to be somewhat nonlinear in either direction and dependent on several factors, including the magnitude of the SLR and coastal geometry to name but two (Lin et al. 2012; Zhang et al. 2013; Bilskie et al. 2016). That is, in some instances/locations, the inundation height because of SLR is greater than the sum of SLR and base storm surge while in other instances/locations, it is less than the sum.

Increases in storm frequency further increase the storm surge AALs by 72% and 123% for the Intermediate-Low and Intermediate-High SLR scenarios respectively as the SLR effectively amplifies the impact from frequency increase (e.g., $1.23 \times 1.41 = \sim 1.72$). The relative contributions of storm surge to the wind and surge AAL, however, changes very little from the SLR results without storm frequency increases, simply because the additional increases to surge loss are countered completely and even a little bit more by increases in wind loss. Recalling the behavior of storm surge loss relative to wind loss in Fig. 8.9, especially for the Gulf Coast Region, adding more major category strength storms does not change the relative contribution of storm surge loss to wind loss very much (there is a very slight decrease).

Impacts from SLR and increases in storm frequency to RP storm surge losses are comparable to or even greater than those for storm surge AAL – approaching a factor of two for the 25-year RP result. The RP results are shown in more detail in Grenier et al. (2020) and are not repeated here. The impacts on the percent contribution from

surge for return period loss results are harder to assess given that a range of events needs to be evaluated and then the average contribution has to be calculated. The results at a county level are also difficult to extract from the software used to compute losses but can be inferred from the base sea level ones. For example, the counties with no storm surge contribution in Fig. 8.9 likely remain that way because they are land-locked, with surge contributions in other counties increasing approximately by one-third and two-thirds for the Intermediate-Low and Intermediate-High SLR scenarios. For the coastally adjacent counties of Brazoria, Chambers, and Galveston, which together contribute nearly one-third to the Houston Region AAL, the percent contributions could increase from roughly 30% to roughly 40% for the intermediate low SLR scenario.

Despite the significant contributions from storm surge to the Houston Region AAL, the bulk of the loss comes from wind (inland flood losses are significant but contribute only half of the wind total). From a mitigation standpoint, it is therefore beneficial to increase resilience to wind in addition to storm surge.

To that end it is worth considering how the RP windspeeds change for the region because of increases in storm frequency. Here, the region is defined by a 5-degree latitude-longitude box surrounding Galveston. Each of the 1000 sub-sampled catalogs for both the current and future climates will yield slightly different results within the box, so it is useful to examine the variability in the results from the sub-sampled catalogs, for both the current and future climates. Figure 8.14 shows how the distributions from the 1000 sub-sampled catalogs for the current and future climates differ for three different return periods. Each graph shows the number of sub-sampled catalogs (vertical axis) that yield a windspeed (horizontal axis) as the return period value. For example, the upper panel shows that for the current climate, the redrawn catalogs show that 2 catalogs have a 10-year return period windspeed value between 55 and 60 mph (not visible), 165 catalogs have a value between 60 and 65 mph, 778 catalogs have a value between 65 and 70 mph, and 55 catalogs have a value between 70 and 75 mph.

The 10-year RP windspeed distribution shows a nearly 5 mph shift from the current to the future climate while higher RP windspeed distributions show a lesser effect from current to future climate as indicated by the broader distributions, although for the 100-year RP, the most probable RP windspeed does shift by a 5-mph band. Additional RP windspeed analyses for the 5-degree $\times$ 5-degree region surrounding Galveston shows that major hurricane strength windspeed occurs for the current climate at around the 30-year RP. Because the future climate frequency is assumed to increase by ~20%, the return period for a major hurricane strength windspeed decreases to about 25 years (30/1.2). The information regarding how RP storm surge inundation heights may change because of SLR and storm activity (latter not shown here) and how RP windspeeds could change is useful for conducting more detailed cost-benefit analyses to determine optimal mitigation strategies including changes in building codes.

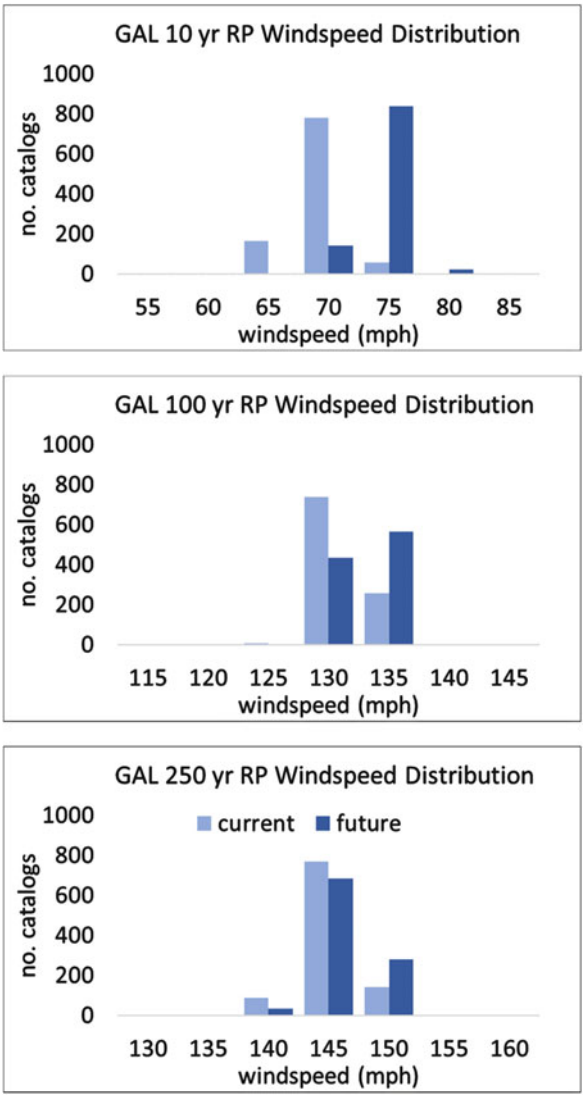

Fig. 8.14 Selected RP surface windspeed distributions for the Galveston-Houston, TX region for current and future climate. Region defined by 5 degree latitude-longitude-longitude box centered on Galveston, TX. Windspeeds are modeled one-minute sustained at 10 m AGL

8.3.6 Miami Return Period Wind and Storm Surge Results

Although not quite as hurricane-prone as Galveston, the Miami region sees a high frequency of hurricane activity (14 landfalls within ~50 nmi of downtown since 1900). For Miami-Dade County, the contribution from storm surge to wind and surge losses, however, is slightly higher (32%) than for any coastal county in the Houston Region examined here, as shown in Fig. 8.15. The reasons for that include (a) Miami, unlike Houston, is located right at the coast, (b) it is an extensively built-

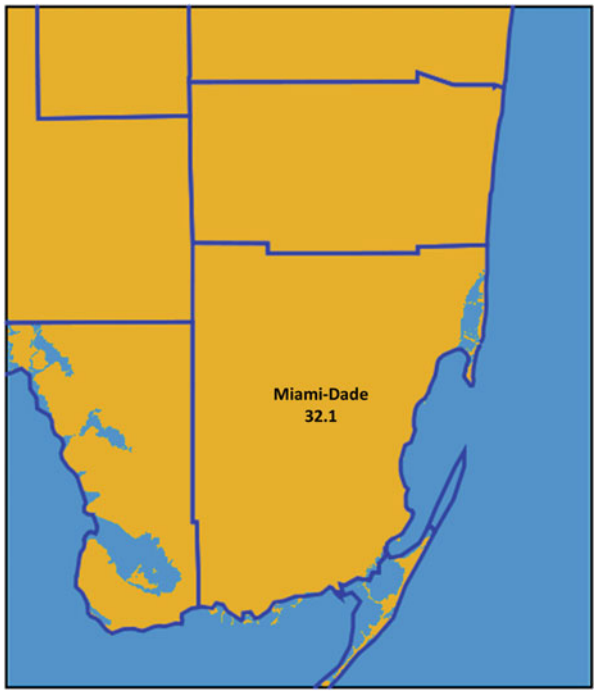

Fig. 8.15 Percent contribution (numbers) of storm surge to wind+surge AAL for Miami-Dade County, Florida for current climate

up region extending inland several tens of kilometers, and (c) the terrain is nearly flat with high water content nearby even under normal conditions because of the Everglades. Figure 8.16 shows selected return period inundation heights for the coastal portion of Miami-Dade County for current sea levels. It is useful to compare the results with the Galveston ones in Fig. 8.10. It is evident that despite the relatively flat terrain of the county as a whole, the stretch of coastal area from Miami northward is mostly spared, although that is not the case for the city of Miami Beach which essentially acts as a barrier island to Miami. South of Miami, even lower elevations (e.g., 2 m or less extending out to Interstate 1) and the presence of the Everglades south and west contribute significantly to the dramatic inland extent of surge. A comparison of Figs. 8.15 and 8.10 and Figs. 8.16 and 8.11 indicates that storm surge contributes more to loss despite the fact that the maximum storm surge inundation heights are lower at all return periods for Miami than for Galveston. While the lower RP storm surge heights may be related to the slightly lower frequency of activity for Miami and the low SLR projections (c.f. Table 8.1), it is more likely related to the steeper bathymetry and lesser degree of concavity of the southern Florida coastline. Not only is Galveston Bay a storm surge enhancing feature, but the entire coastline of Texas is conducive for that as well. The higher percent contribution for Miami could be related to the type of exposure in the county and requires a grid cell level analysis that is beyond the scope of this study.

The increases in storm surge loss from the two SLR scenarios, separately and combined with the increases in storm frequency, as well as the relative storm surge

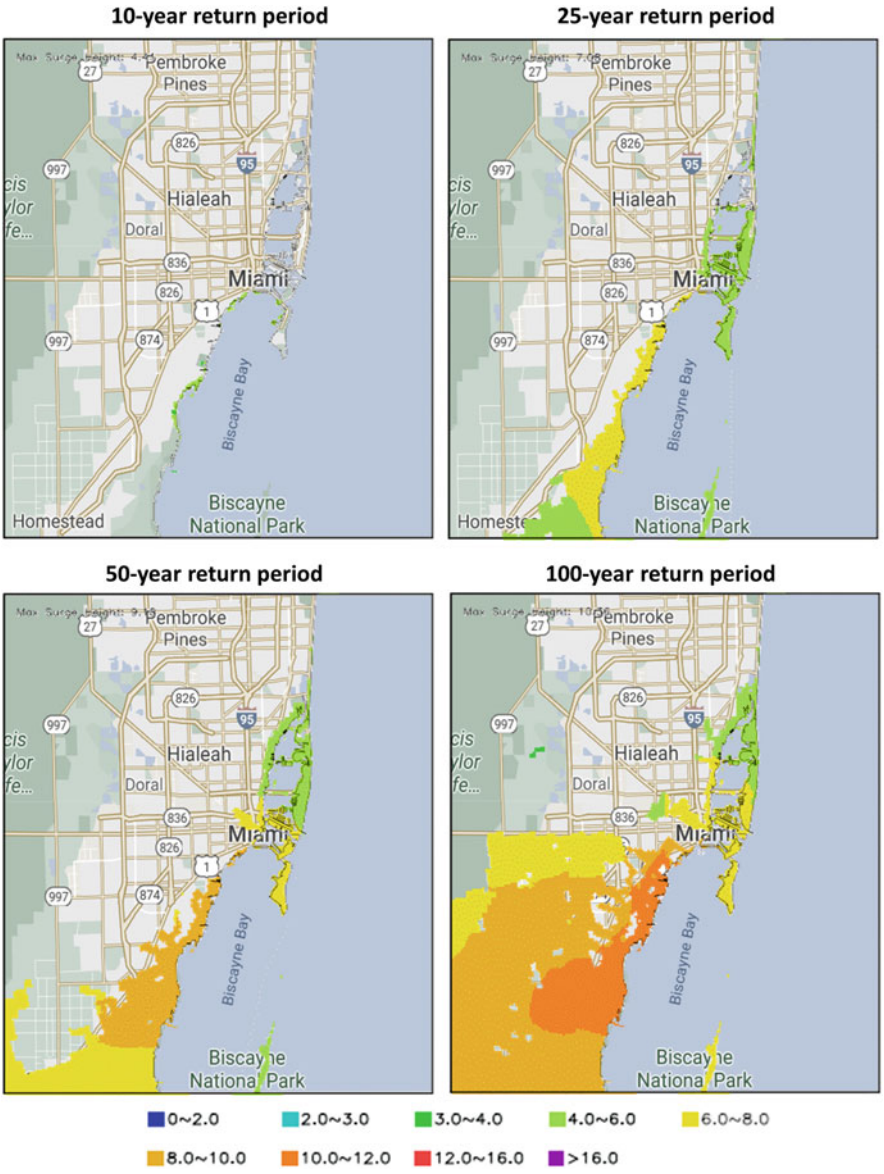

Fig. 8.16 Storm surge inundation height (feet) for Miami Region for return periods and current sea levels. Plotted domain spans 0.60° lat × 0.60° lon

loss compared to wind and surge loss are shown in Table 8.5. The increases in storm surge loss are comparable to those for Galveston, reaching 123% for the Intermediate-High SLR scenario combined with increases in storm activity. One difference is that for the Intermediate-Low SLR scenario, just the SLR by itself

Table 8.5 Summary of impact of SLR and changes in storm frequency on storm surge loss for Miami Region

Scenario	Pct change in surge AAL	Pct contr surge to wind+surge AAL
Current climate	–	32.0
Incr freq	23	32.0
Int-lo SLR scenario	34	38.2
Int-lo SLR scenario + incr freq	64	36.7
Int-hi SLR scenario	83	46.0
Int-hi SLR scenario + incr freq	123	43.8

increases the storm surge loss by about 50% over that for storm activity; and with the 20% increase in storm activity the storm surge loss increase further doubles, resulting in a three-fold increase in storm surge loss from just an increase in storm activity. Recall from Table 8.1 that the projected SLR amounts for Miami are the lowest of the three regions examined in this study, but the increases in the relative contributions from storm surge loss to wind and surge loss are larger than what is shown in the results for Galveston and exceed 40% for the Intermediate-High SLR scenarios (both with and without increases in storm frequency). Finally, we note from Table 8.5 the impact or lack thereof of increased storm frequency on relative contribution of storm surge loss to wind and surge loss. Without SLR, the impact is imperceptible. The addition of SLR amplifies the effect so it is evident to some degree – more so than for the Galveston-Houston Region. The decreased contribution is the result of adding more category 3–5 storms that have smaller relative contributions than their weaker storm counterparts as shown in Fig. 8.9.

Figure 8.17 shows the RP storm surge inundation heights around Miami for select return periods for the two SLR scenarios with increased storm frequency, compared to those for current sea levels. Unlike the situation in Galveston, even the Intermediate-Low SLR scenario shows a dramatic increase in the size of the inundation footprint over that for current conditions, especially at the 50- and 100-year RPs, despite the fact that the sea level increase is the smallest for the three locations. Increase in depths (by virtue of the color changes) are also very evident. Differences in storm surge footprints for the Intermediate-Low scenario are shown in Fig. 8.18 for the 100-year RP, percent changes in footprint sizes are shown for other return periods, and other scenarios are shown in Table 8.6, and maximum storm surge heights for the scenarios at select return periods are shown in Table 8.7. The impacts of SLR and increased storm frequency are considerably larger than for the Galveston Houston Region despite the smaller increases in SLR, although the impacts of increased frequency appear to be less impactful. The increased footprint size from SLR can be attributed to the relative flatness of Miami. Despite the larger impacts on storm surge footprint size, it is difficult to comment on how storm surge losses increase because of changes in footprint size without a much more detailed analysis.

Figure 8.19 shows return period windspeed information for the Miami region in the same format as for Galveston in Fig. 8.14. Note that the return period windspeeds are higher than they are for Galveston (e.g., 10-year RP windspeed is 95 vs. 75 mph)

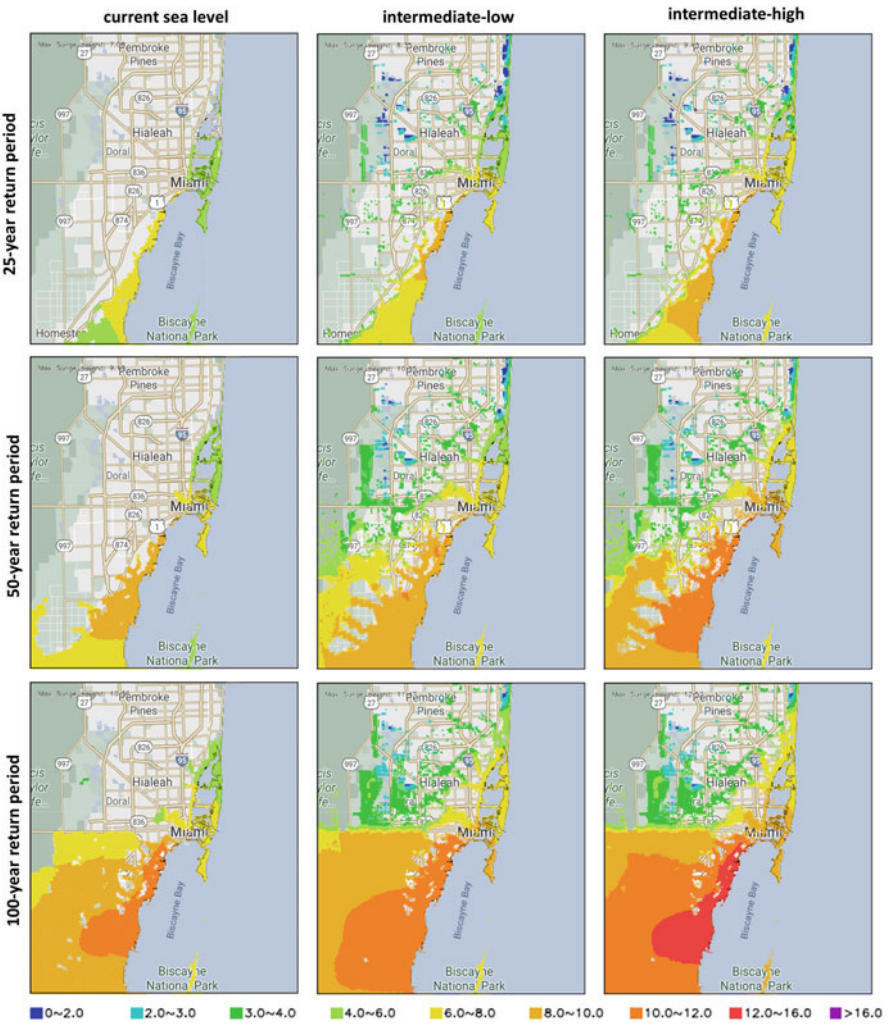

Fig. 8.17 Storm surge inundation heights (feet) for Miami Region for return periods and SLR scenrios as shown. Plotted domain spans 0.60° lat × 0.60° lon

despite the slightly lower storm frequency. Another difference is that there is less impact on the return period windspeeds from the increase in storm activity (note the most probable RP windspeed does not change at the 100- or 250-year RP). The lesser impact suggests that it is the exposure make up (e.g., buildings and contents) and, more specifically, the vulnerability of the buildings in Miami that cause a greater increase in wind loss than storm surge loss for an increase in storm activity.

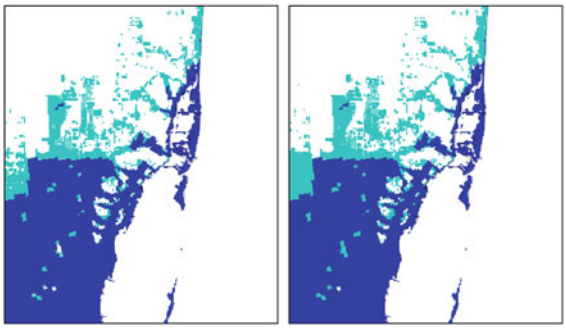

Fig. 8.18 Additional areas inundated (light blue) relative to current sea levels and storm frequency (dark blue) for Intermediate-Lo SLR scenario without frequency increases (left) and for Intermediate-Lo SLR scenario with frequency increases (right) for Miami region for 100 year RP. Base map removed for clarity. Plotted domain spans 0.60° lat × 0.60° lon

Table 8.6 Relative contribution to storm surge footprint area for Miami region for select return periods (top row in years) and for varous climate scenarios

Scenario	1000	500	250	100	50	25	10	5
Base	55,624	54,584	44,366	36,784	20,658	10,543	328	0
Int lo w/o freq incr	5.8	6.2	13.4	**16.2**	28.7	37.3	1062.5	–
Int lo w/ freq incr	6.3	7.0	20.2	**21.5**	54.2	59.3	1473.5	–
Int hi w/o freq incr	6.3	6.9	15.1	17.7	34.0	43.2	1223.5	–
Int hi w/ freq incr	6.9	7.5	21.6	22.8	59.2	65.2	1680.5	–

Numbers for base indicate the numbr of inundated cells for current conditions. Bold numbers correspond to the changes shown in Fig. 8.19

Table 8.7 Maximum storm surge inundation heights (feet) for Miami region for return periods (left column, years) and climate scenarios as shown

RP	Current SLR		Interm low		Interm high	
	w/o freq incr	w freq incr	w/o freq incr	w freq incr	w/o freq incr	w freq incr
5	0.00	0.00	0.63	0.63	1.67	1.67
10	4.41	4.83	5.03	5.45	6.09	6.51
25	7.08	7.72	7.70	8.35	8.76	9.40
50	9.10	9.42	9.73	10.05	10.77	11.10
100	10.36	10.84	10.98	11.47	12.03	12.52
250	11.89	12.34	12.52	12.86	13.56	13.91
500	12.83	13.32	13.45	13.94	14.51	14.99
1000	13.80	14.30	14.43	14.93	15.48	15.98

Current refers to current storm frequency, future refers to increased frequency for major category storms as descibed in the text

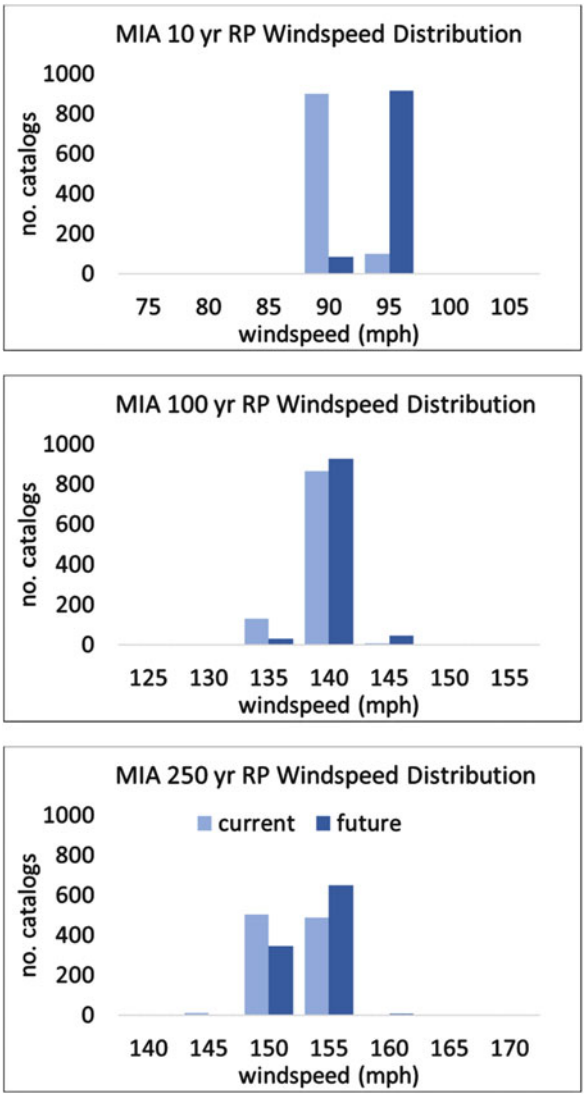

Fig. 8.19 Selected RP surface windspeed distributions for the Miami Region. Region defined by 5 degree latitude-longitude-longitude box centered on Miami, FL

8.3.7 New York City Return Period Wind and Storm Surge Results

Only four hurricanes have made landfall in the New York City Region (50 nmi north or south of southern tip of New York County) since 1900, although many have passed by close enough to cause considerable damage (e.g., Hurricane Sandy in 2012). For this study, all stochastic storms that make landfall between southern Delaware and the northern tip of Long Island, as well as all loss-causing offshore

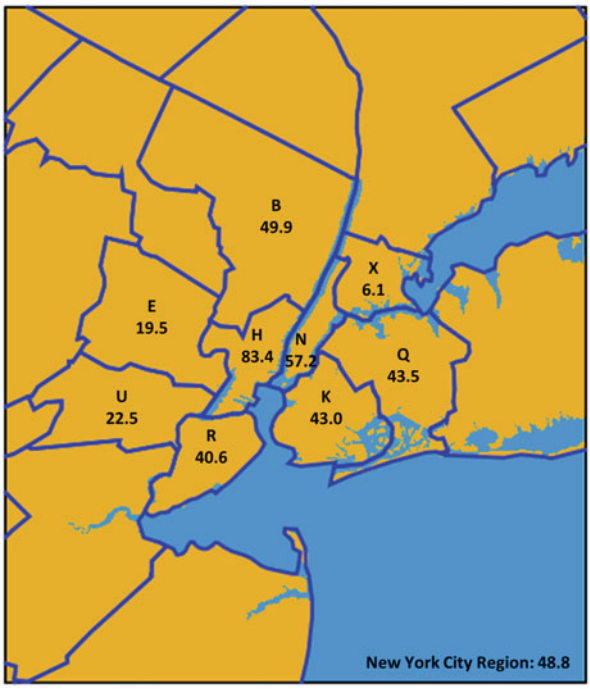

Fig. 8.20 Percent contribution (numbers) of storm surge to wind+surge AAL by county (indicated by first letter except for Bronx) for New York City Region including Bronx, New York, Queens, Kings, Richmond, Bergen, Hudson, Essex, and Union Counties for current climate. Nine county average for New York City Region is 48.8%

bypassing events, are included. Figure 8.20 shows the AIR Modeled result for the contribution of storm surge loss to wind and surge loss. Counties adjacent to the coast or to the Hudson River (where Bergen and Hudson Counties are to the west and New York and Bronx Counties are to the east) have half or more of the loss from storm surge (with the exception of Bronx). The region-average contribution to wind and surge AAL from storm surge is in fact nearly 50%. Like the case with Miami, this very high percentage is the result of exposure locations within the county, although that is where the similarity ends. The New York/New Jersey Coastline in the vicinity of New York City is highly intricate with concave bays, inlets, and narrow rivers nearby. The storm surge return period heights shown in Fig. 8.21 are not as high as what occurs around Miami or Galveston. In fact there is no storm surge footprint from hurricane activity at the 10- or 25- year return period, and storm surge heights are still below 8 feet at the Battery in Manhattan (southrn tip) at the 100-year return period. The high storm surge percentages (Fig. 8.20) come from the fact that wind speeds are also very low (as will be shown), and the buildings are built to withstand strong winds from other more frequent weather phenomena like severe thunderstorms and nor'easters (NYC Emergency Management 2014).

The percent changes in storm surge AAL are shown in Table 8.8 for the SLR scenarios with and without frequency increases. Sea level rise alone increases storm surge AAL by 34–103%.

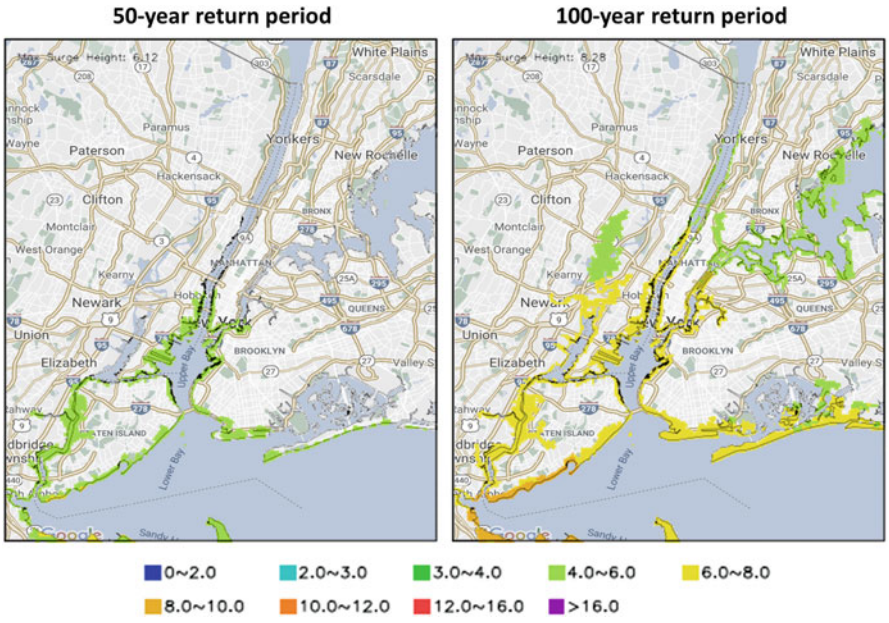

Fig. 8.21 Storm surge inundation height (feet) for Miami region for return periods and current sea levels. Plotted domain spans 0.72° lat × 0.72° lon

Table 8.8 Summary of impact of SLR and changes to storm frequency/intensity on storm surge loss for New York City Region

Scenario	Pct change in surge AAL	Pct contr surge to wind+surge AAL
Current climate	–	48.8
Incr freq	19	48.6
Int-lo SLR scenario	34	55.9
Int-lo SLR scenario + incr freq	64	51.4
Int-hi SLR scenario	103	65.8
Int-hi SLR scenario + incr freq	146	61.6

These are large numbers as well as a very large range, but the results are consistent with the high contributions from the current sea level result. The addition of increases in storm frequency boosts the range to 64–146%. The contribution from storm surge to the wind+surge AAL also increases with SLR: from 48.8% with no SLR to 56% for the Intermediate-Low SLR scenario to 66% for the Intermediate-High SLR scenario. The numbers decrease by several percent with the inclusion of increases in storm frequency. The decreases because of storm activity changes in fact are the largest of the three regions considered. Again, the decreases in relative storm surge contribution may be understood by recalling Fig. 8.9. Given that the northeast region curve is the most concave of all the regions shown, it is easier to see how an

increased frequency of storms with relatively low storm surge contribution would lower the overall relative contribution of storm surge.

Additional understanding to changes in storm surge loss comes from the information in Figs. 8.22 and 8.23 and Tables 8.8 and 8.9. Figure 8.23 ilustrates the impacts of combined SLR and increased storm frequency for the Intermediate-Low and Intermediate-High SLR scenarios for the 50- and 100-year RP footprints. Note that at the 25-year RP, the region is still dry! At the 50-year RP, Manhattan remains dry even for the Intermediate-High SLR scenario. Figure 8.23 shows this more clearly – the increased flood in southern Manhattan is primarily the result of increased storm surge height. Although this is generally true for the region, increased flood area does exist in parts of coastal Long Island and northern New Jersey. Tables 8.9 and 8.10 indicate that significant increases in areal extent occur not only because of SLR but also because of increased storm frequency and have a similar impact on maximum storm surge inundation height.

Table 8.10, for example, shows that for the 100-year RP, the maximum surge height from just an increase in storm frequency is the same as that for just an increase in sea level from the Intermediate-Low scenario.

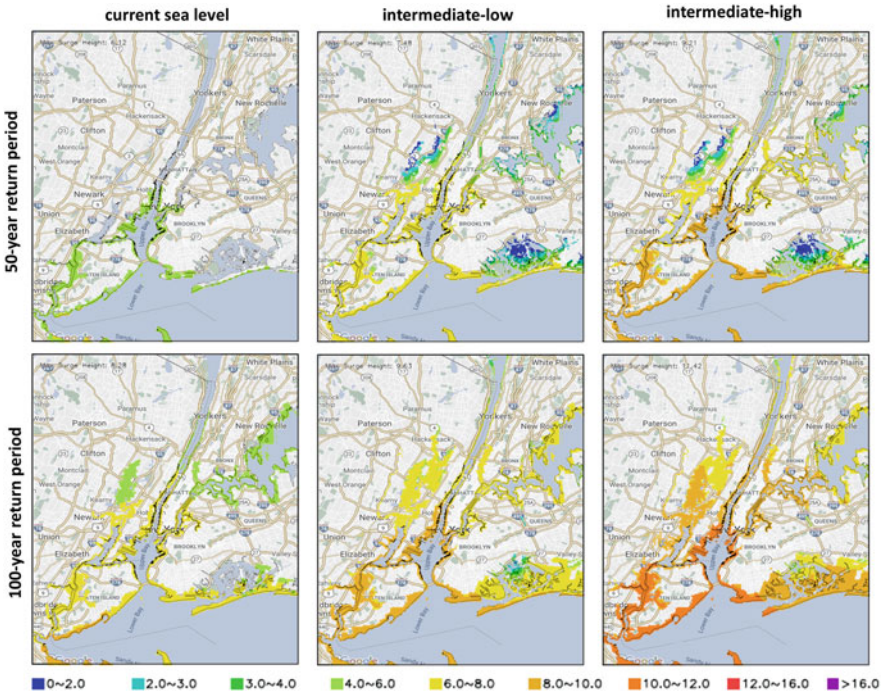

Fig. 8.22 Storm surge inundation heights (feet) for New York City Region for return periods and SLR scenrios as shown. Plotted domain spans 0.72° lat × 0.72° lon

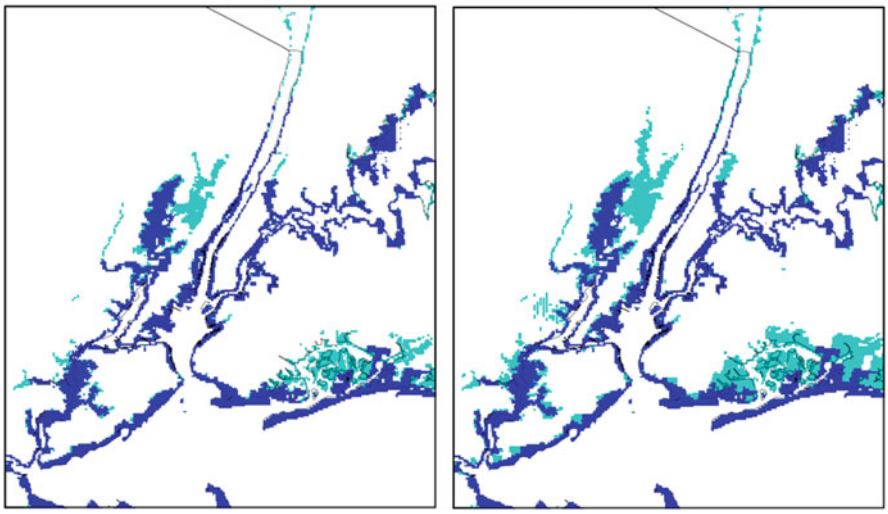

Fig. 8.23 Additional areas inundated (light blue) relative to current sea levels and storm frequency (dark blue) for Intermediate-Hi SLR scenario without frequency increases (left) and for Intermediate-Hi SLR scenario with frequency increases (right) for New York region for 100 year RP. Base map removed for clarity. Plotted domain spans 0.60° lat × 0.60° lon

Table 8.9 Relative contribution to storm surge footprint area for Miami region for select return periods (top row in years) and for varous climate scenarios

Scenario	1000	500	250	100	50	25	10	5
Base	19,138	17,994	16,105	10,277	4151	0	0	0
Int lo w/o freq incr	3.0	3.8	5.0	26.5	112.9	–	–	–
Int lo w/ freq incr	4.3	6.2	8.9	38.9	136.6	–	–	–
Int hi w/o freq incr	3.8	5.1	6.9	**29.7**	120.6	–	–	–
Int hi w/ freq incr	5.6	8.3	12.6	**49.2**	165.2	–	–	–

Numbers for base indicate the numbr of inundated cells for current conditions. Bold numbers correspond to the changes shown in Fig. 8.19

Table 8.10 Maximum storm surge inundation heights (feet) for Miami region for return periods (left column, years) and climate scenarios as shown

RP	Current SLR		Interm low		Interm high	
	w/o freq incr	w freq incr	w/o freq incr	w freq incr	w/o freq incr	w freq incr
5	0.00	0.00	0.00	0.00	0.00	0.00
10	0.00	0.00	0.69	0.69	2.03	2.03
25	0.00	0.00	0.69	0.69	2.03	2.03
50	6.12	6.78	6.81	7.48	8.15	9.21
100	8.28	8.94	8.97	9.63	10.31	11.42
250	10.86	11.74	11.55	12.43	12.89	13.93
500	12.67	13.48	13.36	14.17	14.70	15.81
1000	14.33	14.99	15.02	15.68	16.36	17.32

Current refers to current storm frequency, future refers to increased frequency for major category storms as descibed in the text

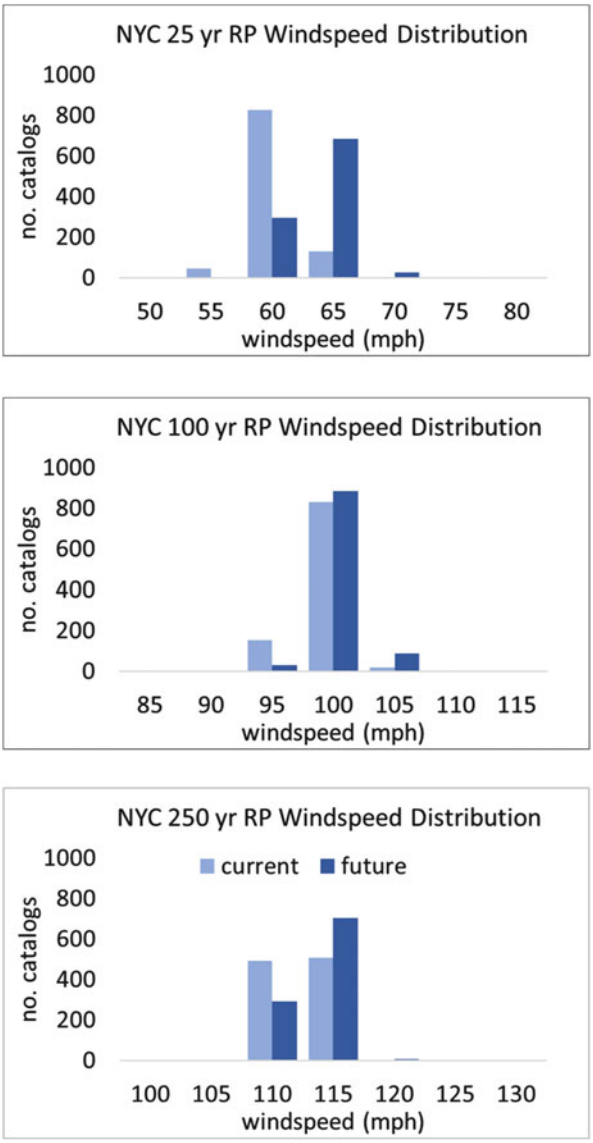

Fig. 8.24 Selected RP surface windspeed distributions for the New York City region. Region defined by 5 degree latitude-longitude-longitude box centered on Newy York City, NY

The New York City region experiences fewer and weaker storms than do the other two regions because of its northern location. Figure 8.24 shows return period windspeed information for the region obtained from this study. The 25-year RP windspeed result shows the most probable windspeed is below hurricane strength (74 mph) for the current climate and for the future climate scenario evaluated here will stay below hurricane strength. Higher RP windspeeds, beginning with the 50-year one (not shown), are above hurricane strength but will likely change less –

only by a couple miles per hour. It is notable that such small increases in windspeed are associated with a 20% increase in wind loss, but it is important to keep in mind that it is the increase in frequency that is really driving the increase – although, because of the way the sub-sampling is performed, the slight increases in intensity (from a return period perspective) are inherently tied to the frequency increase.

8.4 Discussion and Future Work

The loss results in the last section describe some of the potential impacts from climate change on hurricane activity; namely, that there could be a higher frequency of strong (i.e., major category strength) storms. Impacts of climate change on precipitation rate are not accounted for, although changes in precipitation-induced flooding do reflect increased storm frequency. Key Finding #1 from this study is that by mid-century, climate change could result in a 20% increase in U.S. hurricane loss from a 20% increase in Saffir Simpson category three or higher storms (where the categories are defined by landfalling central pressure.) While it seems somewhat coincidental that a twenty percent increase in the frequency of major category storms at landfall leads to an increase in expected loss twenty percent, the result can be explained by the fact that these strong storms contribute to the majority of the loss even though they only account for less than half of landfalling storm activity. It is also related to how the twenty percent increase in major storm frequency is achieved. Table 8.11 summarizes the contributions of various strength storms in terms of frequency and loss for the current climate in the AIR Hurricane Model, as well as for the future climate scenario used in this study.

The simplicity of the result for AAL is an artifact of the implied regional homogeneity for the climate change target used in this study. Moreover, it suggests that other changes to AAL from alternate changes to frequencies of categories can be estimated quickly without the need for generating entire climate change catalogs. For example, even though changes in weak category storms were not imposed as part of

Table 8.11 Summary of current and future climate landfall frequency as defined in this study and annual average loss contribution from all sub-perils for U.S. (percent contribution) by Saffir Simpson category defined in terms of landfalling central pressure

	Category 1	Category 2	Category 3	Category 4	Category 5	Total
Cp range (mb)	≥980	980–965	965–945	945–920	< 920	
Current climate						
Freq contr (%)	15.7	39.4	28.8	13.5	02.6	100.0
Loss contr (%)	01.2	14.9	31.9	38.9	13.1	100.0
Future climate						
Δ freq (%)	00.0	00.0	15.0	25.0	35.0	20.0
Loss contr (%)	01.2	14.9	36.7	48.6	17.7	119.1

For future climate landfall frequency changes are shown. Sea level rise is not included in this result

the climate change target, we can get a credible U.S.-wide estimate of the impacts using the information in Table 8.5 for an assumed reduction in weak storm frequency. A fifteen percent reduction in category 1 storms changes the 119.1% result to 118.9%. Importantly, the catalogs are necessary to evaluate changes in return period losses as well as other aspects of loss and hazard. The catalogs allow an evaluation of how specified changes in the frequencies of different intensities influence regional structure to the sub-peril losses. Finally, the process for creating the catalogs provides a framework by which to evaluate more complex future climate scenarios, e.g., from accounting for changes by region or accounting for changes in forward speed. While it is probably the case that the specific increase depends on how the twenty percent increase is achieved across the major strength storms, it is a straightforward exercise to obtain the range.

An equally important dimension of this study is that it provides information on changes in the relative contributions of storm surge loss from sea level rise. The result is not a simple one that can be accomplished in an excel-spread sheet, nor one that can even be addressed by sub-sampling. In fact, the analysis in this study required the creation of tens of thousands of new events with new storm surge footprints. Key Finding #2 is that sea level rise could likely contribute significantly to increased storm surge loss. Combined with increases from increased storm activity, storm surge loss could more than double, and the contribution of storm surge loss relative to loss from wind will also likely increase, but how much will depend on the amount of sea level rise relative to increases in storm frequency, as well as the geography of the region, and the resilience of the buildings and infrastructure to wind and water damage. Without additional coastal protection, adaptation, or retreat, rising sea levels will impact a larger proportion of land area, population, and global assets in the years ahead (Kirezci et al. 2020). This study has shown how storm surge footprints at different return periods may change because of SLR and because of increased storm frequency. That breakdown can allow a comparison of the relative impacts to loss from areas that already get flooded to those from new areas that get flooded because of SLR and increased storm frequency although it was not shown in this study. The information is of more than just academic interest because insurance companies want to know what new risks they can decide to take on or decline.

Significant utility stems from the second key finding and suggests how insurance underwriting practices may change, how optimal resilience strategies can be developed, and how and where money should be spent to mitigate future risk. Although not presented in this study, changes in the sizes and intensities of storm surge footprints for the different sea level rise scenarios can be evaluated quantitatively from output generated for this study to better inform decisions regarding increased sea-wall protection. Similarly, how to alter building codes to make buildings more resilient along the coast and inland and how much additional cost is involved (e.g., per building) to offset otherwise increased damage from increased storm activity is also information that can be obtained from further analyses.

In obtaining the results, several assumptions were made. The extent to which an extreme scenario like RCP 8.5 will be the emissions pathway that is followed at least

through 2050 is perhaps at the top of the list (although the remainder of the list is not in any particular order of priority). Although it is sometimes referred to as a business-as-usual scenario (e.g., with no additional curbing of greenhouse emissions), it could unfortunately be achieved even with cutting greenhouse gasses if other catastrophic events occur such as collapsing Antarctic ice shelves still occur. That possibility, plus a conservative desire especially from the insurance industry to be prepared for the worst, is the reasoning behind our choice. How tropical cyclone activity responds to climate change is also uncertain. Despite the best science, it is still not known whether the total number of tropical cyclones per year will actually change and how. Although there has been general agreement that the total number of tropical cyclones will decrease, primarily because the number of weak storms is expected to decrease, some recent work has suggested that the total number of tropical cyclones may increase (Lee et al. 2020). Our choice of a climate change target is based on the general consensus that stronger storms will likely become more frequent (Hayhoe et al. 2018). While frequency changes for weaker storms cannot be ignored, we have shown that their contribution to total loss is relatively small, but that analysis assumes that the inland flood contribution from weaker storms does not change disproportionally – e.g., that weaker storms become wetter from slower forward speeds, overall size, etc. – in comparison to stronger storms. We have also made assumptions that relative landfall frequencies will not change, inland decay rates will not change (Li and Chakraborty 2020), storm tracks will not change, forward speeds, etc. will not change. Additionally, we did not account for potential changes in precipitation rate from climate change. While these may not be immaterial, there may be less confidence in how they will change relative to frequency or intensity. Lastly, we note potential limitation of the results from the subsampling approach used, that it is possible that future climate change may yield 10,000-year storms that are not contained within our 100,000-year catalog of current climate storms.

We plan to address potential changes in these other storm characteristics noted above and how they may affect loss in future studies. We also plan to complete the detailed sea level rise – storm surge analysis for the rest of the U.S. hurricane-affected coastline. The latter will include a more detailed evaluation of how footprint sizes change.

Acknowledgements We gratefully acknowledge the many comments and suggestions from two anonymous reviewers on an earlier draft of this manuscript.

References

AIR (2008) Climatological influences on hurricane activity: the AIR warm SST conditioned catalog. Available from: https://www.air-worldwide.com/SiteAssets/Publications/White-Papers/documents/Climatological-Influences-on-Hurricane-Activity%2D%2DThe-AIR-Warm-SST-Conditioned-Catalog

AIR (2021) The AIR hurricane model for the U.S. V1.0.0 as implemented in Touchstone® 2020: submitted in compliance with the 2019 standards of the Florida Commission on Hurricane Loss

Projection Methodology May 19, 2021. 452 pp. Available from The State Board of Administration, Tallahassee

Bacmeister JT, Reed KA, Hannay C et al (2018) Projected changes in tropical cyclone activity under future warming scenarios using a high-resolution climate model. Clim Change 146:547–560. https://doi.org/10.1007/s10584-016-1750-x

Bilskie MV, Hagen SC, Alizad K, Medeiros SC, Passeri DL, Needham HF, Cox A (2016) Dynamic simulation and numerical analysis of hurricane storm surge under sea level rise with geomorphologic changes along the northern Gulf of Mexico. Earth's Future 4:177–193. https://doi.org/10.1002/2015EF000347

Caesar L, McCarthy GD, Thornalley DJR, Cahill N, Rahmstorf S (2021) Current Atlantic Meridional Overturning Circulation weakest in last millennium. Nat Geosci 14:118–120

Camargo SJ (2013) Global and regional aspects of tropical cyclone activity in the CMIP5 models. J Clim 26:9880–9902. https://doi.org/10.1175/JCLI-D-12-00549.1

DeConto RM, Pollard D (2016) Contribution of Antarctica to past and future sea-level rise. Nature 531:591–597

Emanuel K (2021) Response of global tropical cyclone activity to increasing CO2: results from downscaling CMIP6 models. J Clim 34:57–70

Emanuel K, DesAutels C, Holloway C, Korty R (2004) Environmental control of tropical cyclone intensity. J Atmos Sci 61:843–858

Evans JL (1993) Sensitivity of Tropical Cyclone Intensity to Sea Surface Temperature. J Climate 6:1133–1140. https://doi.org/10.1175/1520-0442(1993)006<1133:SOTCIT>2.0.CO;2

Frederikse T, Landerer F, Caron L et al (2020) The causes of sea-level rise since 1900. Nature 584: 393–397. https://doi.org/10.1038/s41586-020-2591-3

Grenier R, Sousounis P, Schneyer J, Raizman D (2020) Quantifying the impact from climate change on U.S. hurricane risk. AIR Worldwide, 44 pp. Available from: How climate change could impact U.S. hurricane risk | Visualize | Verisk Analytics

Hall TM, Kossin JP (2019) Hurricane stalling along the North American coast and implications for rainfall. NPJ Clim Atmos Sci 2:17. https://doi.org/10.1038/s41612-019-0074-8

Harris DL (1957) The hurricane surge. Coast Eng Proc 1:5. https://doi.org/10.9753/icce.v6.5

Hayes C, Rowe J (2008) The AIR industry exposure databases. AIR Curr Oct 2008. https://www.air-worldwide.com/SiteAssets/Publications/AIR-Currents/attachments/AIR-Currents%2D%2DIED

Hayhoe K, Wuebbles DJ, Easterling DR, Fahey DW, Doherty S, Kossin JP, Sweet W, Vose R, Wehner M (2018) Our changing climate. In: Reidmiller DR, Avery CW, Easterling DR, Kunkel KE, Lewis KLM, Maycock TK, Stewart BC (eds) Impacts, risks, and adaptation in the United States: fourth national climate assessment, volume II. U.S. Global Change Research Program, Washington, DC, 72:144. https://doi.org/10.7930/NCA4.2018.CH

Hofer S, Lang C, Amory C et al (2020) Greater Greenland Ice Sheet contribution to global sea level rise in CMIP6. Nat Commun 11:6289. https://doi.org/10.1038/s41467-020-20011-8

IPCC (2013) Climate change 2013: the physical science basis. In: Stocker TF, Qin D, Plattner G-K, Tignor M, Allen SK, Boschung J, Nauels A, Xia Y, Bex V, Midgley PM (eds) Contribution of Working Group I to the fifth assessment report of the Intergovernmental Panel on Climate Change. Cambridge University Press, Cambridge and New York, p 1535. https://doi.org/10.1017/CBO9781107415324

Jelenianski CP, Chen J, Shaffer WA (1992) SLOSH: Sea, lake, and overland surges from hurricanes; NOAA technical report NWS 48; National Oceanic and Atmospheric Administration, U.S. Department of Commerce, Silver Spring, pp 1–71

Kirezci E, Young IR, Ranasinghe R, Muis S, Nicholls RJ, Lincke D, Hinkel J (2020) Projections of global-scale extreme sea levels and resulting episodic coastal flooding over the 21st century. Sci Rep 10:11629. https://doi.org/10.1038/s41598-020-67736-6

Knutson TR, Sirutis JJ, Vecchi GA, Garner S, Zhao M, Kim H-S, Bender M, Tuleya RE, Held IM, Villarini G (2013) Dynamical downscaling projections of twenty-first-century Atlantic

hurricane activity: CMIP3 and CMIP5 model-based scenario. J Climate 26:6591–6617. https://doi.org/10.1175/JCLI-D-12-00539.1

Knutson TR, Sirutis JJ, Zhao M, Tuleya RE, Bender MA, Vecchi GA, Villarini G, Chavas D (2015) Global projections of intense tropical cyclone activity for the late twenty-first century from dynamical downscaling of CMIP5/RCP4.5 scenarios. J Climate 28. https://doi.org/10.1175/JCLI-D-15-0129.1

Knutson TR, Camargo SJ, Chan JCL, Emanuel K, Ho C, Kossin JP, Mohapatra M, Satoh M, Sugi M, Walsh K, Wu L (2019) Tropical cyclones and climate change assessment: part I. Detection and attribution. Bull Am Meteor Soc 100. https://doi.org/10.1175/BAMS-D-18-0189.1

Knutson TR, Camargo SJ, Chan JCL, Emanuel K, Ho C, Kossin JP, Mohapatra M, Satoh M, Sugi M, Walsh K, Wu L (2020) Tropical cyclones and climate change assessment: part II. Projected response to anthropogenic warming. Bull Am Meteor Soc 10. https://doi.org/10.1175/BAMS-D-18-0194.1

Kopp RE, Horton RM, Little CM, Mitrovica JX, Oppenheimer M, Rasmussen DJ, Strauss BH, Tebaldi C (2014) Probabilistic 21st and 22nd century sea-level projections at a global network of tide gauge sites. Earth's Future 2:287–306. https://doi.org/10.1002/2014EF000239

Kossin JP (2018) A global slowdown of tropical cyclone translation speed. Nature 558:104–107

Kossin JP, Emanuel KA, Vecchi GA (2014) The poleward migration of the location of tropical cyclone maximum intensity. Nature 509:349–352

Lee C-Y, Camargo SJ, Sobel AH, Tippett MK (2020) Statistical-dynamical downscaling projections of tropical cyclone activity in a warming climate: two diverging genesis scenarios. J Clim 33:4815–4834. https://doi.org/10.1175/JCLI-D-19-0452.1

Li L, Chakraborty P (2020) Slower decay of landfalling hurricanes in a warming world. Nature 587:230–234. https://doi.org/10.1038/s41586-020-2867-7

Lin N, Emanuel K, Oppenheimer M, Vanmarcke E (2012) Physically based assessment of hurricane surge threat under climate change. Nat Clim Change 2462–2467. https://doi.org/10.1038/NCLIMATE1389

Little CM, Horton R, Kopp R et al (2015) Joint projections of US East Coast sea level and storm surge. Nat Clim Change 5:1114–1120

Liu M, Vecchi GA, Smith JA, Knutson TR (2019) Causes of large projected increases in hurricane precipitation rates with global warming. NPJ Clim Atmos Sci 2:38. https://doi.org/10.1038/s41612-019-0095-3

Lonfat M, Marks FD, Chen SS (2004) Precipitation distribution in tropical cyclones using the tropical rainfall measuring Mission (TRMM) microwave imager: a global perspective. Mon Wea Rev 132:1645–1660. https://doi.org/10.1175/1520-0493(2004)132<1645:PDITCU>2.0.CO;2

McInnes KL, Macadam I, Hubbert G, O'Grady J (2013) An assessment of current and future vulnerability to coastal inundation due to sea-level extremes in Victoria, southeast Australia. Int'l J Climatol 33:33–47

NAIC (2017) CIPR study: flood risk and insurance. Available online: https://content.naic.org/sites/default/files/inline-files/cipr_study_1704_flood_risk.pdf

NOAA Tides and Currents (2021). https://tidesandcurrents.noaa.gov/sltrends/sltrends.html

NYC Emergency Management (2014) New York City's risk landscape: a guide to hazard mitigation, 172 pp. Available online: nycs_risk_landscape_a_guide_to_hazard_mitigation_final.pdf

Pielke RA, Gratz J, Landsea CW, Collins D, Saunders MA, Musulin R (2008) Normalized hurricane damages in the United States: 1900–2005. Nat Hazards Rev 9:29–42

Roberts MJ, Camp J, Seddon J, Vidale PL, Hodges K, Vannière B, Mecking J, Haarsma R, Bellucci A, Scoccimarro E, Caron L-P, Chauvin F, Terray L, Valcke S, Moine M-P, Putrasahan D, Roberts CD, Senan R, Zarzycki C, Ullrich P, Yamada Y, Mizuta R, Kodama C, Fu D, Zhang Q, Danabasoglu G, Rosenbloom N, Wang H, Wu L (2020) Projected future changes in tropical cyclones using the CMIP6 HighResMIP multimodel ensemble. Geophys Res Lett 47:e2020GL088662. https://doi.org/10.1029/2020GL088662

Robinson E, Cipullo M, Sousounis P, Kafali C, Latchman S, Higgs S, Maisey P, Mitchell L (2017) UK windstorms and climate change. An Update to ABI Research Paper No. 19, 2009. pp 18. Available online: https://www.abi.org.uk/globalassets/files/publications/public/property/2017/abi_final_report.pdf

Schwalm CR, Glendon S, Duffy PB (2020) RCP8.5 tracks cumulative CO2 emissions. Proc Natl Acad Sci 117:19656–19657

Sealya K, Strobl E (2017) A hurricane loss risk assessment of coastal properties in the Caribbean: Evidence from the Bahamas. Ocean Coast Manag 149:42–51

Sweet WV, Kopp RE, Weaver CP, Obeysekera J, Horton RM, Thieler ER, Zervas C (2017) Global and regional sea level rise scenarios for the United States. NOAA technical report NOS CO-OPS 083. NOAA/NOS Center for Operational Oceanographic Products and Services

Ting M, Kossin JP, Camargo SJ, et al. (2019) Past and future hurricane intensity change along the U.S. East Coast Sci Rep 9:7795. https://doi.org/10.1038/s41598-019-44252-w

USACE (2020) Economic guidance memorandum (EGM) 01-03, generic depth damage relationships. U.S. Army Corps of Engineers Memorandum, CECWPG4, Washington, DC

Villarini G, Vecchi GA (2013) Projected increases in North Atlantic tropical cyclone intensity from CMIP5 models. J Climate 26:3231–3240

Zhang K, Yi L, Liu H, Xu H, Shen J (2013) Comparison of three methods for estimating the sea level rise effect on storm surge flooding. Climatic Change 118:487–500. https://doi.org/10.1007/s10584-012-0645-8